

| | | | | | |
|--|--|---|---|--|-----------|
| 1. Report No. FHWA/TX-06/0-4774-2 | | 2. Government Accession No. | | 3. Recipient's Catalog No. | |
| 4. Title and Subtitle FIELD EVALUATION OF NEW TECHNOLOGIES FOR MEASURING PAVEMENT QUALITY | | | | 5. Report Date December 2005 Resubmitted: March 2006 Published: April 2006 | |
| | | | | 6. Performing Organization Code | |
| 7. Author(s) Tom Scullion, Stephen Sebesta, Daniel Rich, and Wenting Liu | | | | 8. Performing Organization Report No. Report 0-4774-2 | |
| 9. Performing Organization Name and Address Texas Transportation Institute The Texas A&M University System College Station, Texas 77843-3135 | | | | 10. Work Unit No. (TRAIS) | |
| | | | | 11. Contract or Grant No. Project 0-4774 | |
| 12. Sponsoring Agency Name and Address Texas Department of Transportation Research and Technology Implementation Office P. O. Box 5080 Austin, Texas 78763-5080 | | | | 13. Type of Report and Period Covered Technical Report: September 2004-August 2005 | |
| | | | | 14. Sponsoring Agency Code | |
| 15. Supplementary Notes Project performed in cooperation with the Texas Department of Transportation and the Federal Highway Administration. Project Title: New Technologies and Approaches to Controlling the Quality of Flexible Pavement Construction URL:http://tti.tamu.edu/documents/0-4774-2.pdf | | | | | |
| 16. Abstract Traditional quality control testing of new pavement layers typically consists of localized random testing of layer density. In this process less than 1 percent of the pavement area is tested. In Project 0-4774, the focus in the second year of the project was to develop and evaluate two technologies, which provide close to 100 percent coverage of the section under construction. The first technology is instrumented rollers where an accelerometer is placed on the drum of a standard steel wheel vibratory roller. A prototype system was developed which can be mounted on any traditional vibratory roller. The complete system consists of an accelerometer, a distance-measuring device and specialized software for data acquisition, processing, and display. Field tests were conducted with this prototype unit, and it was demonstrated that the roller displacements are directly related to the quality of support of the foundation layer. Weak spots in the foundation layer can be detected with this system. The roller displacements were not correlated to the density measurements in the upper layers. The roller movements were correlated to traditional stiffness measuring systems such as the Dynamic Cone Penetrometer and Portable Falling Weight Deflectometer (FWD). The second technology is infrared testing to identify low temperature spots in newly placed layers of asphalt. A prototype infrared bar was evaluated in this project. The bar can be attached to the foot plate at the back of the paver. Specialized software displays in real time the temperature profile of the new asphalt layer. More field testing is recommended for both devices. For the infrared system a draft specification was developed for consideration of inclusion in TxDOT's Quality Control/Quality Assurance (QC/QA) program. | | | | | |
| 17. Key Words Quality Control, Quality Assurance, Flexible Pavements, Infra-red, Segregation, Intelligent Compaction, Roller Mounted Compaction Control | | | 18. Distribution Statement No restrictions. This document is available to the public through NTIS: National Technical Information Service Springfield, Virginia 22161 http://www.ntis.gov | | |
| 19. Security Classif.(of this report) Unclassified | | 20. Security Classif.(of this page) Unclassified | | 21. No. of Pages 68 | 22. Price |

FIELD EVALUATION OF NEW TECHNOLOGIES FOR MEASURING PAVEMENT QUALITY

by

Tom Scullion, P.E.
Research Engineer
Texas Transportation Institute

Stephen Sebesta
Research Associate
Texas Transportation Institute

Daniel Rich, P.E.
Graduate Assistant Research
Texas Transportation Institute

and

Wenting Liu, P.E.
Associate Research Engineer
Texas Transportation Institute

Report 0-4774-2

Project 0-4774

Project Title: New Technologies and Approaches to Controlling the Quality
of Flexible Pavement Construction

Performed in cooperation with the
Texas Department of Transportation
and the
Federal Highway Administration

December 2005

Resubmitted: March 2006

Published: April 2006

TEXAS TRANSPORTATION INSTITUTE
The Texas A&M University System
College Station, Texas 77843-3135

DISCLAIMER

The contents of this report reflect the views of the authors, who are responsible for the facts and the accuracy of the data presented herein. The contents do not necessarily reflect the official views or policies of the Texas Department of Transportation or the Federal Highway Administration. The United States Government and the State of Texas do not endorse products or manufacturers. Trade or manufacturers' names appear herein solely because they are considered essential to the object of this report. This report does not constitute a standard, specification, or regulation. The engineer in charge was Tom Scullion, P.E. (Texas, # 62683).

ACKNOWLEDGMENTS

This project was made possible by the Texas Department of Transportation and the Federal Highway Administration. Special thanks must be extended to Mike Arellano, P.E., for serving as the project director, and Lynn Passmore, P.E., for serving as the program coordinator. The following project advisors also provided valuable input throughout the course of the project:

- Darlene Goehl, P.E.
- James Klotz, P.E.
- Frank Phillips, P.E.
- Walter Smith, P.E.

TABLE OF CONTENTS

| | Page |
|--|-------------|
| List of Figures | viii |
| List of Tables | x |
| Chapter 1. Introduction | 1 |
| Chapter 2. Development of a Prototype Instrumented Roller System..... | 5 |
| Summary of Instrumented Rollers Work..... | 5 |
| Prototype System Development..... | 5 |
| Data Acquisition and Display | 9 |
| Chapter 3. Field Evaluation of Prototype Instrumented Roller | 15 |
| Field Testing Program..... | 15 |
| Field Results from Riverside Campus | 17 |
| Demonstration of Instrumented Roller on SH 21 Near Caldwell..... | 25 |
| Summary of Findings from Instrumented Roller..... | 33 |
| Chapter 4. Development of a New Infrared Imaging System for Hot-Mix Asphalt Overlays | 35 |
| Summary..... | 35 |
| Desired Features of Infrared System..... | 35 |
| Overview of the Current Pave-IR System | 36 |
| Closer Details of Pave-IR System Components | 38 |
| Chapter 5. Example Data from Pave-IR | 43 |
| Summary | 43 |
| Results from Type D HMA in Paris District | 43 |
| Type D HMA in Fort Worth District | 45 |
| Type D HMA on US 90 in Houston District | 46 |
| Chapter 6. Conclusions and Recommendations..... | 49 |
| References..... | 53 |
| Appendix: Draft Specification for IR Testing | 55 |

LIST OF FIGURES

| Figure | Page |
|--|------|
| 1. Prototype Compaction System..... | 6 |
| 2. Accelerometer Mounted on Roller Frame | 6 |
| 3. Lab Calibration of Accelerometer | 7 |
| 4. Mounting of Signal Conditioner on Body of Roller | 8 |
| 5. Distance Measuring Device | 8 |
| 6. Plot of Roller Movement (mm) versus Distance | 10 |
| 7. Power Spectrum of Roller Displacements | 10 |
| 8. Roller Movement Where the Roller Is Jumping Off the Ground | 11 |
| 9. Roller Displacements versus Distance along Project..... | 12 |
| 10. Average Deflection Profile for a Typical Section..... | 13 |
| 11. DCP Testing..... | 15 |
| 12. Nuclear Testing..... | 16 |
| 13. Portable FWD Used for Soil Stiffness Determination..... | 16 |
| 14. Preliminary Field Testing of Instrumented Roller | 17 |
| 15. Roller Movements from Five Replicate Runs on Warehouse Road..... | 18 |
| 16. Average Roller Displacement for Each Pass | 19 |
| 17. Relationship between Roller Movement and Backcalculated Subgrade Modulus | 21 |
| 18. Comparison of Roller Displacement and pFWD Subgrade Modulus..... | 22 |
| 19. Second Test Location at Riverside Campus | 23 |
| 20. Plot of High and Low Amplitude Displacements Around Running Track..... | 23 |
| 21. Average Roller Deflections for Each 25 ft Segment of the Test Track | 24 |
| 22. Testing of TxDOT Construction Project on SH 21 | 25 |
| 23. Roller Displacement Along the Length of Test Section..... | 26 |
| 24. Typical Plots of Measured versus Computed Resilient Modulus..... | 30 |
| 25. Design Idea for Infrared Sensor Bar (<i>I</i>) | 36 |
| 26. TTI's Current Pave-IR System Collecting Project Data..... | 38 |
| 27. Infrared Sensor Installed in Blackbody Source for Calibration..... | 39 |

LIST OF FIGURES (Continued)

| Figure | Page |
|---|------|
| 28. Master Control Box for Pave-IR..... | 40 |
| 29. Sensor Side and Internal Sides of Temperature Bar | 41 |
| 30. Example Thermal Profile from Initial Paving Operation on US 82 | 44 |
| 31. Example Thermal Profile from Modified Paving Operation on US 82 | 44 |
| 32. Histogram of Measured Mat Placement Temperatures from Initial Paving Operation on US 82 | 44 |
| 33. Histogram of Measured Mat Placement Temperatures from Modified Paving Operation on US 82 | 45 |
| 34. Hot Spots from Burner Operation on Idle Paver | 45 |
| 35. Location of Pave-IR Testing on US 90 in August 2005 | 46 |
| 36. Increase in Mean Placement Temperatures on US 90 | 47 |
| 37. Location of Paver Stop on US 90 Eastbound..... | 47 |

LIST OF TABLES

| Table | | Page |
|--------------|---|-------------|
| 1. | Raw Data from Test Site..... | 20 |
| 2. | Backcalculated Moduli for Test Location..... | 20 |
| 3. | pFWD Data..... | 27 |
| 4. | DCP Results for SH 21 Soil Sample Points..... | 27 |
| 5. | Troxler and Calculated Wet and Dry Densities and Moisture Contents..... | 28 |
| 6. | Resilient Modulus Testing Protocol..... | 29 |
| 7. | Resilient Moduli..... | 31 |
| 8. | Atterberg Limits..... | 31 |
| 9. | Roller Displacement versus DCP Penetration Rate..... | 32 |
| 10. | Roller Displacement versus Lab Resilient Modulus..... | 32 |
| 11. | Roller Displacement versus Pocket Penetrometer Su..... | 32 |
| 12. | Roller Displacement with Nuclear Density Readings..... | 32 |
| 13. | Key Pave-IR Hardware Specifications..... | 37 |

CHAPTER 1

INTRODUCTION

The current Texas Department of Transportation (TxDOT) methodology of establishing and controlling compaction of pavement layers is based on adequate in-place density. TxDOT bases its quality assessment on localized nuclear density readings and core results. In several cases, density-control methodology using nuclear gauges has proven to be unreliable and provides insufficient insight on whether the parameters of the pavement design were achieved. In addition, regulations pertaining to nuclear gauges have been tightened, which make it difficult to manage the storage, usage, and transport of the device. Given the deficiency of the density-control methodology, at the initiation of Project 0-4774, it was understood that new methodologies to measure construction quality must be explored. Furthermore, these new devices and techniques will attempt to confirm if design parameters, such as layer stiffness, are being achieved during construction.

In recent years, alternative non-destructive test (NDT) devices have become available. These devices are often based on the principles of seismic, radar, lasers, infrared, and other technologies. TxDOT has made a substantial investment in many of these technologies and has collected a considerable amount of test data and information on these devices. The practicability of utilizing these NDT devices for construction control requires validation. In Project 0-4774, alternative methods, not including seismic technology, were evaluated to measure the quality of flexible pavement layers during construction with the ultimate objective of finding technologies to replace or supplement current density measuring techniques.

In year 1 of Project 0-4774 ([Sebesta et al. 2004](#)) researchers evaluated a number of new technologies to determine the existence of an acceptable replacement to traditional density measuring systems. For density measurement on soils and bases researchers found no new devices to directly replace nuclear density gauges. The sand cone test and Corps of Engineers tube samples were found to be acceptable alternatives, but very labor intensive. For asphalt materials the Pavement Quality Indicator (PQI) and Pavetracker units provided reasonable measurements of density, but they were thought not to be as reliable as the nuclear density gauge. Also, they appeared to have problems on coarse textured surfaces. For moisture

measurements, several alternative devices were reported in the 0-4774-1 report, including the Speedy Moisture meter, Vertek probe, and others.

In presenting the results of the year 1 evaluation to the project steering committee, it was concluded that no new technologies are available to directly replace nuclear density gauges, particularly for soils and bases. However, one major concern was that current random testing programs utilizing the nuclear density testing gauge, or other spot testing devices, typically measure less than 1 percent of the section. If major improvements are to be made to construction quality then a method to quickly and reliably measure the quality of as close to 100 percent of each layer is needed. It was determined that the second year of this project would focus on evaluating technologies, which can test as close as possible to 100 percent of the section. Two technologies in year 2 of this project:

- 1) instrumented rollers for testing subgrade and base materials, and
- 2) infrared sensors for checking the temperature profiles of new asphalt layers.

The instrumented roller technology has been under development in Europe for the past two decades. [Chapter 2](#) presents a summary of these findings. Until recently, this technology has not been available in the United States. However, in the past three years various roller manufacturers have conducted localized demonstrations of their systems. This technology is available from roller manufacturers, such as Bomag and Ammann, who will sell rollers equipped with the necessary instrumentation and display systems. The instrumentation includes an accelerometer and distance-measuring system together with a data processing and display system. However, the packages cannot be purchased separately, and they are only included as an optional feature when purchasing new rollers. In [Chapter 2](#), efforts to develop a package that could be installed onto any vibratory smooth drum roller to measure roller displacement as it compacts soil and base materials. The developed system was used on two pavement sections inside Texas Transportation Institute (TTI's) Riverside Campus and on one TxDOT project on SH 21, where the changes in roller movement were compared with results from other strength testing equipment such as dynamic cone penetrometer (see [Chapter 3](#)).

The infrared system was first proposed in Project 0-4126 ([Sebesta and Scullion 2002](#)). It was built to identify areas of large variations in asphalt layers directly behind a paver. The

implication is that large temperature differentials, particularly cold spots, will be difficult to compact and will provide low-density areas that will permit moisture to enter the low pavement layers. The system proposed in Project 0-4126 was initially field tested as a stand-alone unit, which is pushed behind the lay down machine. However, this push-behind unit was not practical for full-scale implementation, consequently an infrared bar that can be attached to a paver was developed and field tested in this project. The development of the new infrared bar is described in [Chapter 4](#), and the results from field trials are given in [Chapter 5](#). The infrared system is ready for full-scale evaluation, and the feedback from TxDOT districts and paving contractors has been positive. A draft specification for infrared testing is given in the [Appendix](#) to this report.

CHAPTER 2

DEVELOPMENT OF A PROTOTYPE INSTRUMENTED ROLLER SYSTEM

SUMMARY OF INSTRUMENTED ROLLERS WORK

Research studies to use instrumented vibratory rollers as a means of checking compaction started in the late 1970s with the work of Bomag in Germany, Ammann in Switzerland, and Geodynamik in Sweden. The earliest paper on the topic in English was published by [Forssblad \(1988\)](#), and it dealt with research results as well as experience from the field. Forssblad reported on successful studies conducted in Germany where the roller was used to locate weak spots and to avoid over-compaction of subgrade materials.

In the late 1980s several companies started building roller systems with feedback loops where the vibration of the roller would be controlled by sensors installed on the drum. This led to the development of a series of tools with the title “Intelligent Compaction.” The latest tools and equipment available can be located at the following web sites, www.dynapac.com, www.hammag.com, and www.ammann-group.com.

The systems used in Europe and sold by these companies consist of basically an accelerometer, which is attached to the drum of the roller, a distance measuring device, a data acquisition system which converts the accelerometer data into drum displacements, and a display system, which identifies weak areas in the soil under test. In most cases the data is reported in terms of a soil stiffness parameter, which is typically obtained by correlating the roller displacements to insitu soil stiffness, which is measured using traditional test equipment. In Germany the tradition calibration is made with plate bearing equipment.

PROTOTYPE SYSTEM DEVELOPMENT

One limitation of the existing technology is that these systems cannot be purchased separately and mounted on any existing rollers. They are supplied by the manufacturers as options when purchasing a new roller. Consequently, in this project efforts were undertaken to develop an instrumentation kit and the associated software that could be attached to any vibratory smooth drum roller.

During the course of TxDOT Project 0-4774, the prototype system shown in [Figure 1](#) was developed. This accelerometer-based system permits the measurement of drum movements as the drum traverses soil or base material. The system will allow for evaluation of approximately 100 percent of each lift of material for potential compliance with the compaction specifications. A brief description of each of the system components follows.



Figure 1. Prototype Compaction System.

An accelerometer is mounted onto the roller frame, as shown in [Figure 2](#). The accelerometer is positioned between the vibrating drum and the rubber isolation mounts so that only the deflection of the drum is measured.



Figure 2. Accelerometer Mounted on Roller Frame.

The accelerometer used in these initial studies is a Bruel and Krael (B&K) triaxial charge type accelerometer (Type 4321). Prior to installing the system on the roller, the accelerometer and the associated data acquisition system are calibrated in the laboratory. The calibration arrangement is shown in Figure 3 where an exciter of known frequency and amplitude is used to test the accelerometer. The signal from the accelerometer is passed through a signal conditioner that amplifies and double integrates the signal to provide sensor displacement. The charge amplifier box (Type 2635) from B&K can provide output of acceleration, velocity, or displacement. For the test conducted in this project, roller displacement was read directly by the data acquisition system.

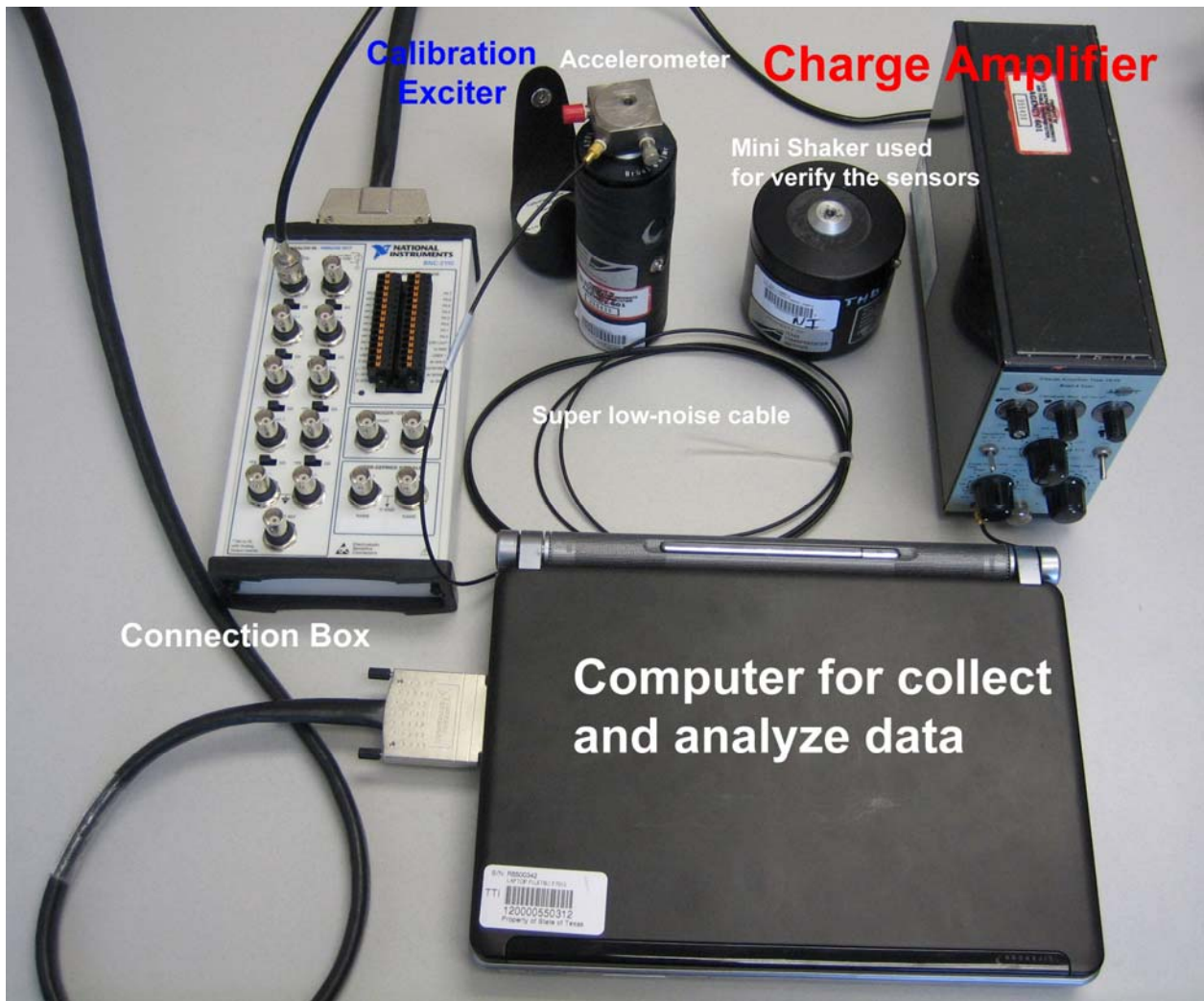


Figure 3. Lab Calibration of Accelerometer.

In the field, the accelerometer is attached as shown in [Figure 3](#). The signal conditioner is housed in a padded box attached to the roller as shown in [Figure 4](#). This is a temporary arrangement which will be modified in future development efforts.



Figure 4. Mounting of Signal Conditioner on Body of Roller.

The position of the roller along each test path is tracked by a distance measuring instrument (DMI) attached to one of the drive wheel hubs ([Figure 5](#)). Calibration of the DMI is required at the start of testing and is accomplished by running the roller along a known distance. Several methods of attaching the DMI have been attempted, with varying degrees of success. Differences in the design of wheel hubs between roller manufacturers limit the development of a standard mounting bracket. Other mounting methods, which do not involve the wheel hub, are being pursued.



Figure 5. Distance Measuring Device.

DATA ACQUISITION AND DISPLAY

The data acquisition system consists of a laptop computer, a National Instruments A/D card (DAQCard-6062E), and custom-built software to collect, process, and display the measured data. The displacement and distance location information is sampled 500 times every second. The raw roller displacement data from one of the runs of the system are shown in the upper plot of [Figure 6](#). This is a plot of drum movement versus distance along the project. This signal consists of two superimposed waveforms. Low frequency displacements, between 0 and 3 Hz, are caused by the movement of the roller over the natural ground and are an indication of the roughness of the surface. From [Figure 6](#) it is clear that high-frequency drum movements (30 Hz) are superimposed on these low-frequency displacements. It is these high-frequency displacements that are an indication of the quality of the support beneath the roller. To decompose these signals, the data is processed through a Fast Fourier Transform (FFT), and the frequency distribution plot shown in [Figure 7](#) is produced. The X-axis is frequency in Hertz, and the Y-axis is a function of the amplitude of the signal at each frequency. From this distribution it is clear that the signal, in the upper part of [Figure 6](#), consists of two clusters of frequencies. One cluster from 0 to 3 Hz is the movements induced in the drum as it drives over the rough ground, and the cluster around 30 Hz is the drum displacement during compaction of the soil as the roller operates at a nominal frequency of 30 Hz. To separate the two components, a band pass filter is applied to the data. Once this is performed a plot of roller displacement with distance is developed, as shown in the lower plot of [Figure 6](#). Once the low frequencies associated with ground roughness are removed, the motion of the roller can be measured.

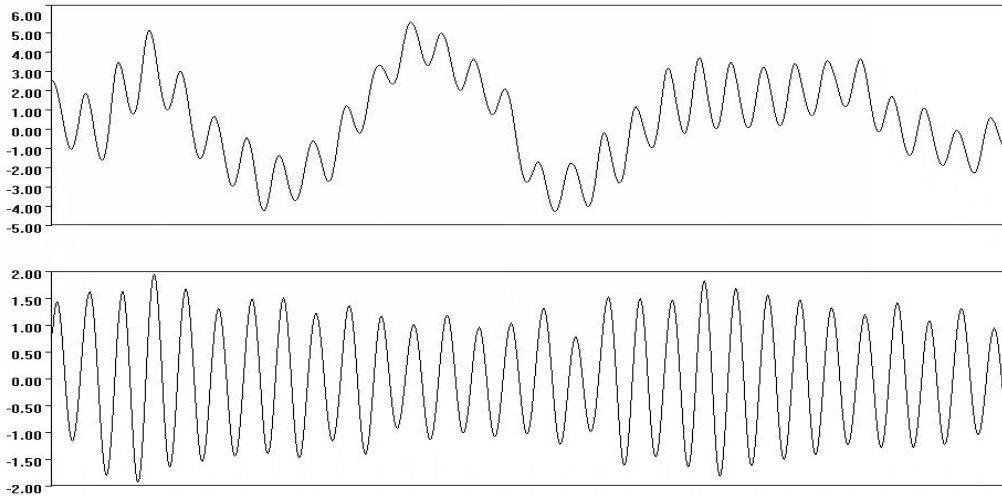


Figure 6. Plot of Roller Movement (mm) versus Distance. The upper graph is typical roller movement including section roughness and roller vibrations. When the roughness is removed (lower graph) the roller movement is observed.

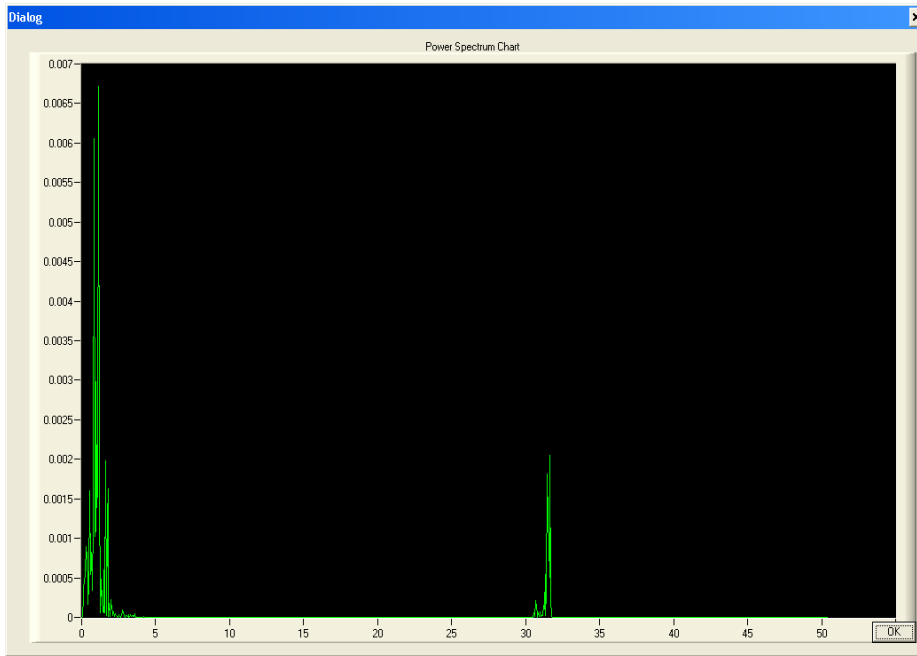
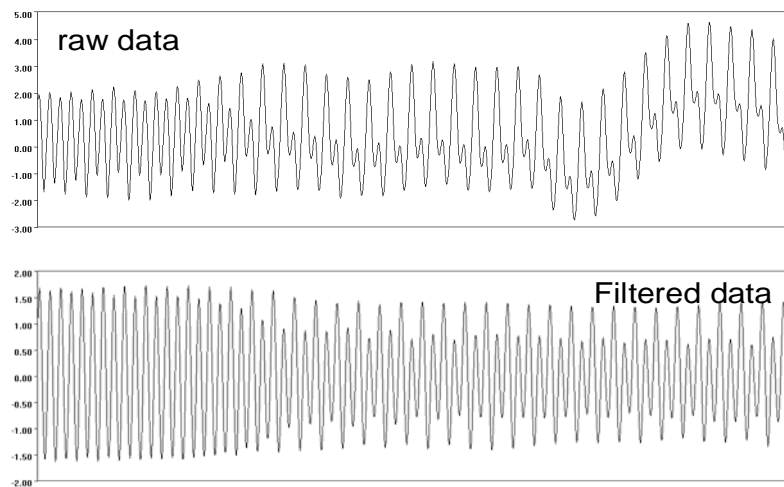


Figure 7. Power Spectrum of Roller Displacements. (Power versus Frequency)

The deflection pattern shown in the lower graph of [Figure 6](#) is judged as ideal. The peak to peak amplitudes show the true motion of the roller in contact with the soil being compacted. Variations in this amplitude will be studied in the [next chapter](#) of this report. However, on very stiff materials such as cement stabilized base or asphalt surfacing a different deflection pattern was observed with these roller tests ([Figure 8](#)). The upper part of the figure is the raw data, and the lower plot shows the motion of the drum. This lower plot shows a non-consistent set of amplitudes. This pattern is associated with cases where the roller is no longer in contact with the layer surface, and the roller is jumping off the ground. In all subsequent studies it was necessary to adjust the roller controls (frequency/amplitude) so that displacement patterns similar to [Figure 6](#) (rather than [Figure 8](#)) were obtained.



Typical signal (raw & filtered)

Figure 8. Roller Movements Where the Roller Is Jumping Off the Ground.

The final step in the data acquisition system is to measure the amplitudes (peak to peak) and display them against distance along the project. [Figure 9](#) shows a typical roller displacement plot. From this plot it is observed that low movements were observed at distances of 50 and 150 feet from the start of the run. The cause of these variations will be discussed in the [next chapter](#) of this report.

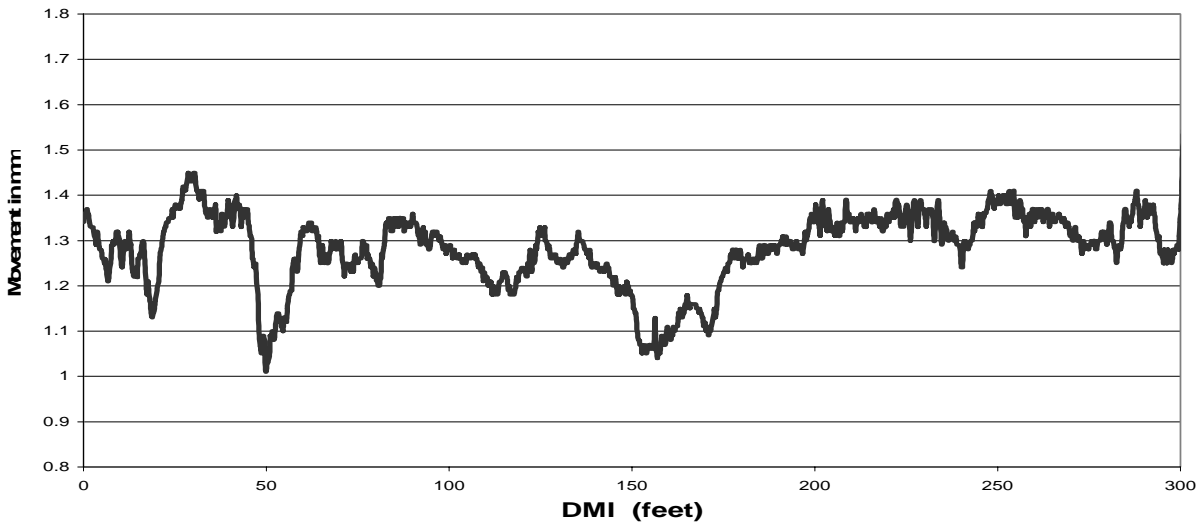


Figure 9. Roller Displacements versus Distance along Project.

Plots such as that shown in [Figure 9](#) form the basis of using roller mounted compaction meters in future projects. For any application it will be necessary to establish threshold criteria for acceptable and unacceptable movements. In Europe the next step would be to correlate the low and high spots in the deflection profile with stiffness or density measurements made with other devices (such as plate bearing or dynamic cone tests). In the case of the data shown in [Figure 9](#) calibration tests would be made at two low spots (50 and 150 ft) and two high spots (for example 30 and 250 ft), so that threshold values can be obtained.

The final step in the data analysis is to process the roller displacement data into standard reporting intervals such as 25 ft so that areas requiring additional work can be clearly defined. For example if 1.1 mm was defined as the deflection threshold then a distribution similar to that shown in [Figure 10](#) could be inspected to easily identify possible problem areas. In this case areas 7 and 8 fall below the threshold values and require additional compaction.

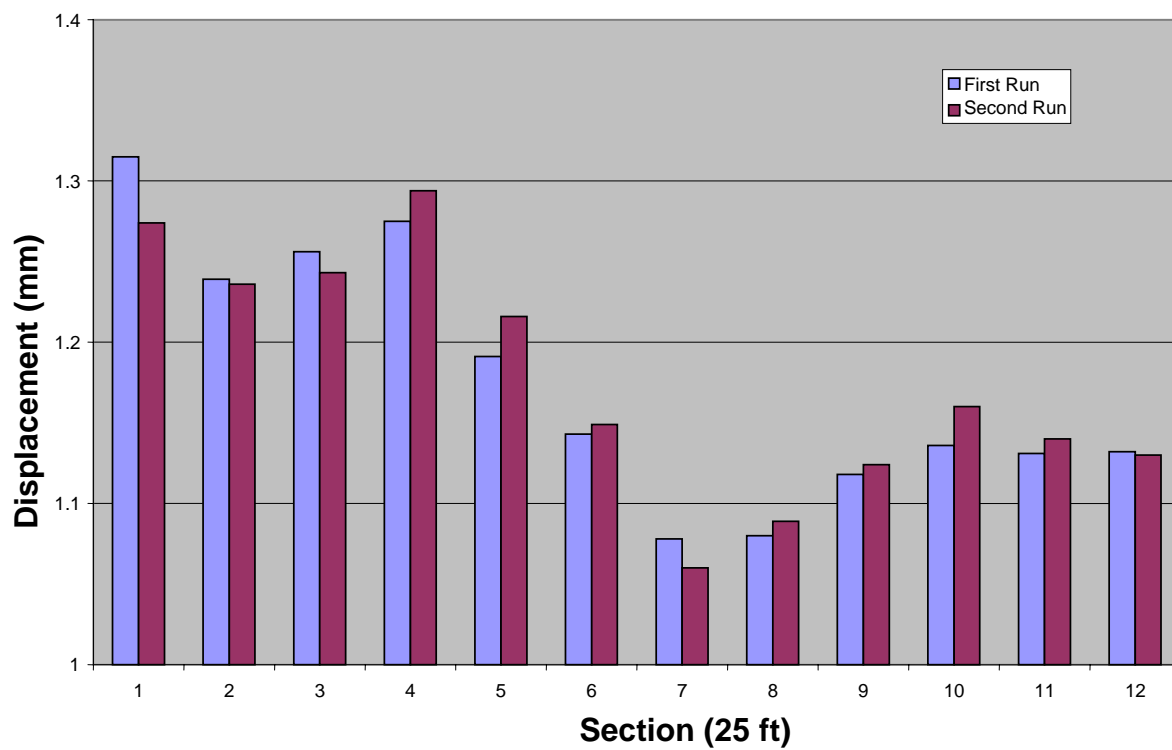


Figure 10. Average Deflection Profile for a Typical Test Section.

CHAPTER 3

FIELD EVALUATION OF PROTOTYPE INSTRUMENTED ROLLER

A series of field and laboratory tests were conducted to validate the prototype system and to evaluate how changes in roller displacement compare with soil properties measured with the traditional equipment. Researchers conducted testing at Texas A&M University's Riverside Campus and on a TxDOT road project on SH 21 near Caldwell. Shelby tube samples were also taken at selected areas on the SH 21 site so that laboratory tests could be conducted to determine insitu soil properties.

FIELD TESTING PROGRAM

On each of the projects tested with the instrumented roller "ground truth" data was also collected with one or more of the following devices:

1. Dynamic Cone Penetrometer (DCP): The DCP, shown in [Figure 11](#), measures the soil's resistance to penetration for a calibrated amount of impact energy provided by a falling weight. Analysis of the data defines layers within the test depth by revealing break points or changes in the slope of the penetration rate.



Figure 11. DCP Testing.

2. Nuclear gauge: The nuclear gauge, shown in [Figure 12](#), measures wet and dry density and moisture content of the soil down to approximately 12 inches below the soil surface by means of a radioactive source.



Figure 12. Nuclear Testing.

3. Portable Falling Weight Deflectometer (pFWD): The pFWD, shown in [Figure 13](#), is a much smaller version of the FWD that measures vertical displacement of the soil surface at three points due to a vertical impact load. A back calculated modulus is also determined.



Figure 13. Portable FWD Used for Soil Stiffness Determination.

The purpose of the staged field tests was to test different components and configurations and to identify shortcomings or weaknesses that could limit the system's data-gathering ability. Modifications (major and minor) were made to the system after each test.

FIELD RESULTS FROM RIVERSIDE CAMPUS

On June 24, 2005, the system was tested on a section of gravel road that ran perpendicular to Warehouse Road at Texas A&M's Riverside Campus. [Figure 14](#) shows the section.



Figure 14. Preliminary Field Testing of Instrumented Roller.

The main purpose of the testing was to determine how to install the system onto a vibratory smooth drum roller (CAT CS 433E—operating at 30 HZ) and to make sure that the system would collect data. Multiple passes were made across the same section of road with good repeatability (see [Figure 15](#)). The graphs of drum displacement with distance had very similar shapes, which indicated that the system was consistently measuring the same soil property. Additionally, the roller displacement at each point generally increased with each pass, which was consistent with an improvement in the strength of the material.

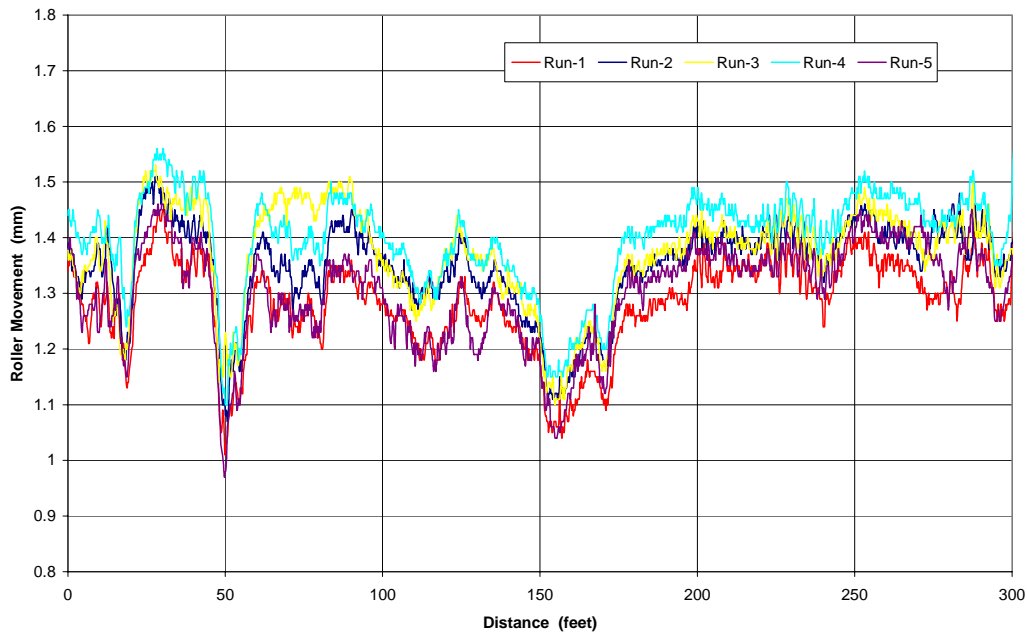


Figure 15. Roller Movements from Five Replicate Runs on Warehouse Road.

As shown in [Figure 16](#), the average movement of the roller increased with each pass. It was initially assumed that the drum of the instrumented roller would move more when it was testing softer soils, which turned out not to be the case. It was determined that at these high frequencies of loading (30 Hz) the softer the soil the lower the amplitude of roller movement. At the extreme case of very stiff sections, the roller will actually come close to bouncing off the ground. At these spots, the amplitude of motion will be very large. On weak soils the roller stays in full contact with the soil, and most of the energy of the roller is transferred into the soil. This relationship between roller motion and soil stiffness was found on all sections tested in this project when the roller was operating at a frequency of around 30 Hz, which is the normal operating frequency for most vibratory rollers. However, limited work was conducted with a low-frequency roller, operating at 8 Hz, and in that case the relationship reversed. Softer soil had more roller movement. It is assumed that below the resonant frequency of soil that one relationship exists, with a different relationship above the resonant frequency. More work is needed in this area. However, as most existing rollers operate in the frequency range of 25 to 35 Hz, the relationship of increasing roller movement with increasing soils stiffness can be assumed.

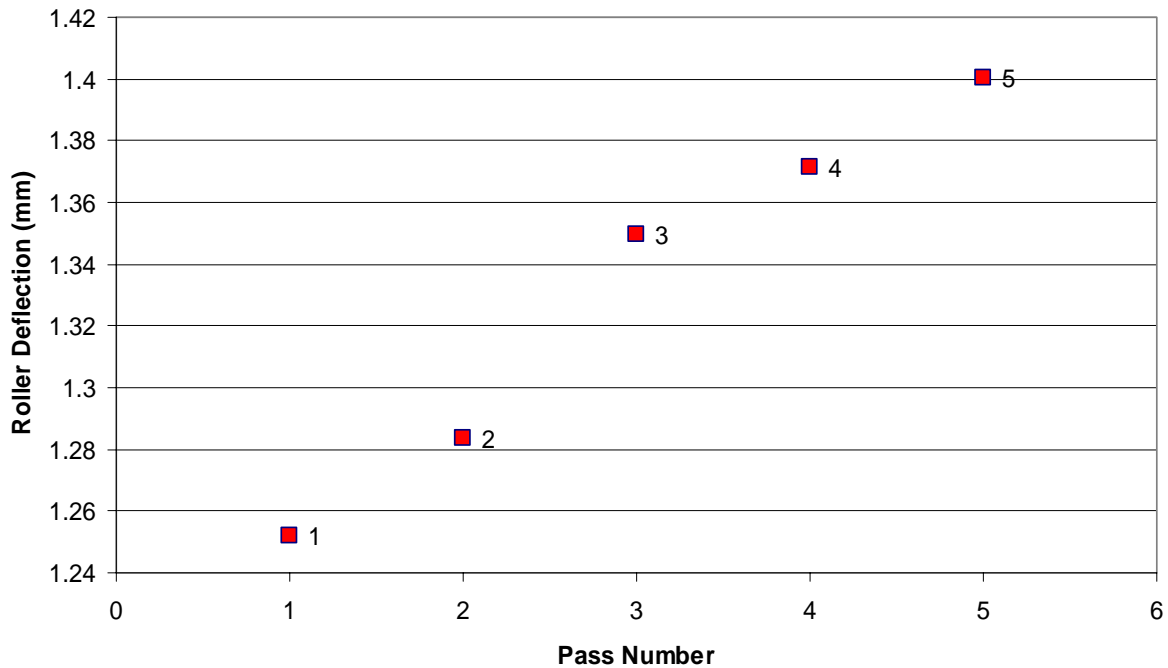


Figure 16. Average Roller Displacement for Each Pass.

On this test location, the existing pavement has 8 to 10 inches of gravel base over a raw clay subgrade. DCP tests were conducted at selected points of high and low roller displacement and at points of intermediate displacement. DCP testing was conducted at four locations 50, 75, 100, and 158 ft from the start of the section. On the first two locations, the DCP was used to test only the top 10 inches of the structure. At the last two locations, DCP testing tested both the base and top of subgrade to a depth of 24 inches.

In addition, portable FWD tests (Figure 13) were conducted at approximately 25 ft intervals along this project. Table 1 shows the combined data set for the four DCP locations.

Table 1. Raw Data from Test Site.

| Location (feet) | Roller Displacement (mm) | DCP in/blow | | Portable FWD | | | |
|-----------------|--------------------------|-------------|----------|--------------|---------------------|---------------------|---------------------|
| | | 0-10 in | 10-24 in | Load (lb) | d ₁ (mm) | d ₂ (mm) | d ₃ (mm) |
| 50 | 1.17 | 0.133 | - | 1973 | 9.02 | 2.2 | 0.91 |
| 75 | 1.45 | 0.099 | - | 1957 | 5.31 | 2.2 | 1.02 |
| 100 | 1.36 | 0.137 | 1.05 | 1964 | 8.74 | 2.28 | 1.06 |
| 158 | 1.10 | 0.180 | 1.29 | 1957 | 12.8 | 4.06 | 1.81 |

The portable FWD data from this project was processed using a modified version of Modulus 6 (Liu and Scullion 2001). In this version, the three channels of deflection and the load levels were input, and the back calculated stiffness for the base and subgrade was computed.

Table 2 shows the computed stiffness for the pFWD data.

Table 2. Backcalculated Moduli for Test Location (* hit low limit for value).

| Location (feet) | Roller Displacement (mm) | Portable FWD Modulus (ksi) | |
|-----------------|--------------------------|----------------------------|----------|
| | | Base | Subgrade |
| 50 | 1.17 | 30.9 | 12.1 |
| 75 | 1.45 | 47.3 | 20.4 |
| 100 | 1.36 | 23.6 | 17.7 |
| 158 | 1.10 | 20* | 11.2 |

From the results given in Table 2 it appears that the roller movements are correlated with subgrade modulus values. The relationship from Table 2 is shown graphically in Figure 17.

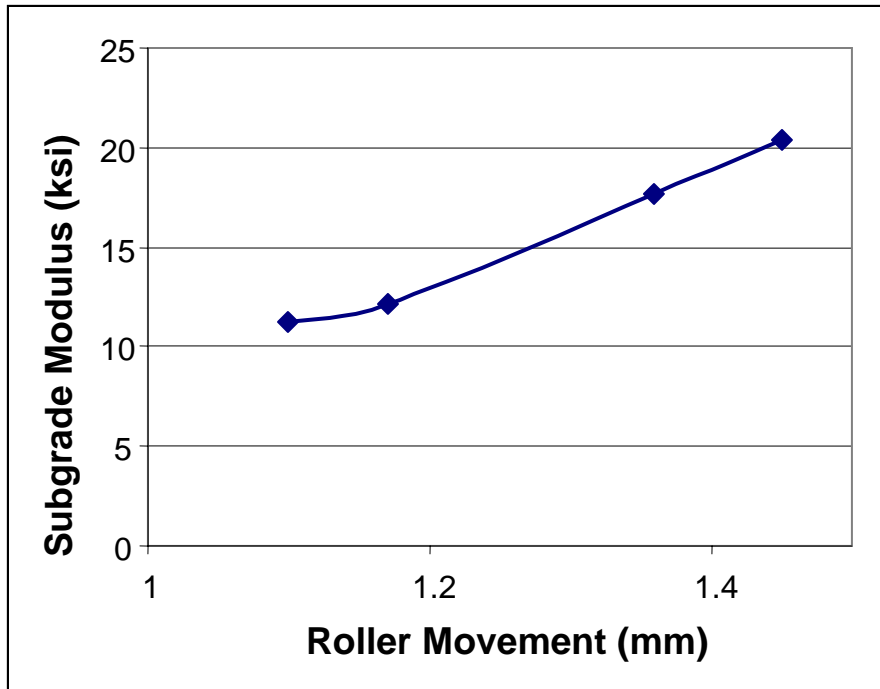


Figure 17. Relationship between Roller Movement and Back calculated Subgrade Modulus.

The relationship between roller movement and subgrade modulus for the entire test section is shown graphically in [Figure 18](#). There is good agreement between roller movement and the subgrade support value. The conclusion from this test is that the roller displacements are an indication of the overall structural support, however they may not be a good indicator of the level of compaction of the upper lift of the structure.

To be used on any project it will be necessary to develop a relationship such as that shown in [Figure 17](#). The designer would specify a minimum acceptable subgrade modulus (say 12 ksi) and from [Figure 17](#) the equivalent roller movement would be define (for example 1.1mm). It would then be possible to run the entire project and investigate all potential problem areas where the roller movements were less than 1.1 mm. At these locations DCP testing could be undertaken to identify the cause of the low support values.

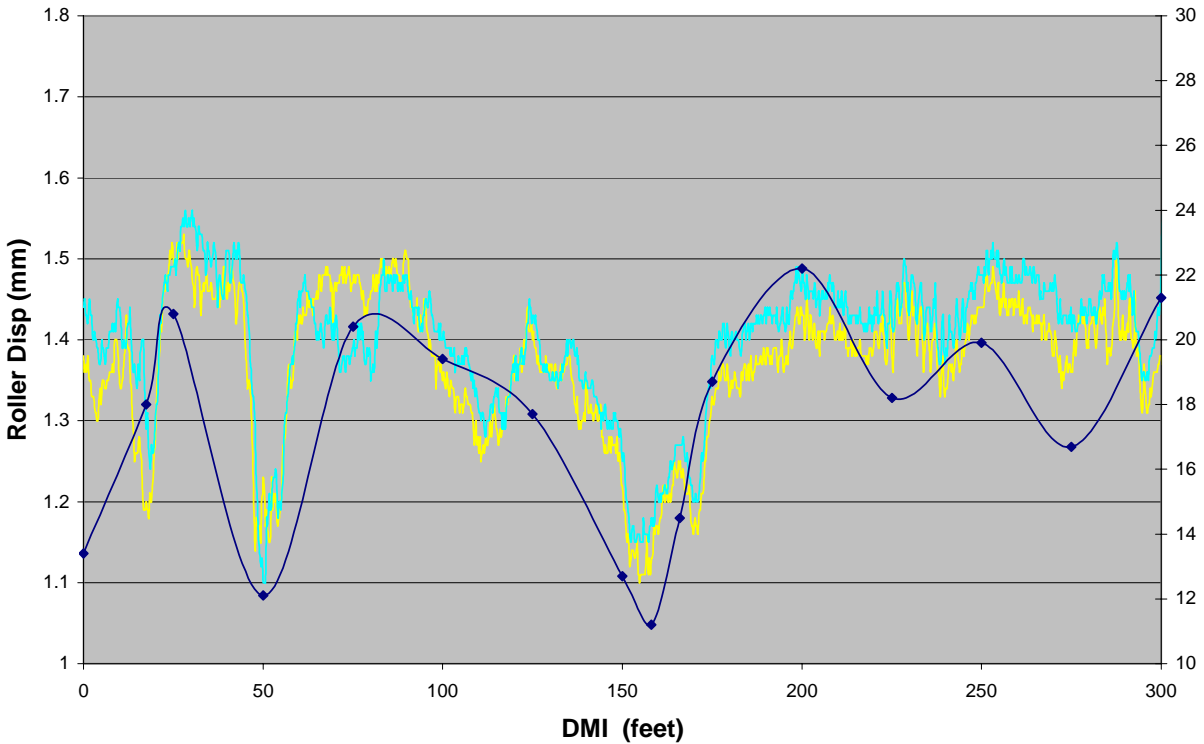


Figure 18. Comparison of Roller Displacement and pFWD Subgrade Modulus (blue line) (scale on right axis is pFWD subgrade modulus (ksi)).

Testing a New Running Track (July 2005, Riverside Campus)

A 1/4 mile long running track was under construction during the testing. The contractor gave TTI permission to test the system on the partially compacted subgrade. As shown in [Figure 19](#) evidence of the weak areas included: shoving of the soil by the roller drum, imprint of roller's tires into the surface, and imprint of the testing staff's boot heels into the surface. The first test of the system was conducted on low amplitude vibration mode, and the second was tested on high amplitude vibration mode. The system easily distinguished between the visibly weaker and stronger areas as evidenced by the magnitude of the roller drum displacements regardless of the mode, as shown below in [Figure 20](#). The photographs show two stronger areas and one clearly weaker area; again it was found that the low roller displacement correlates with the poor soil support.



Figure 19. Second Test Location at Riverside Campus.

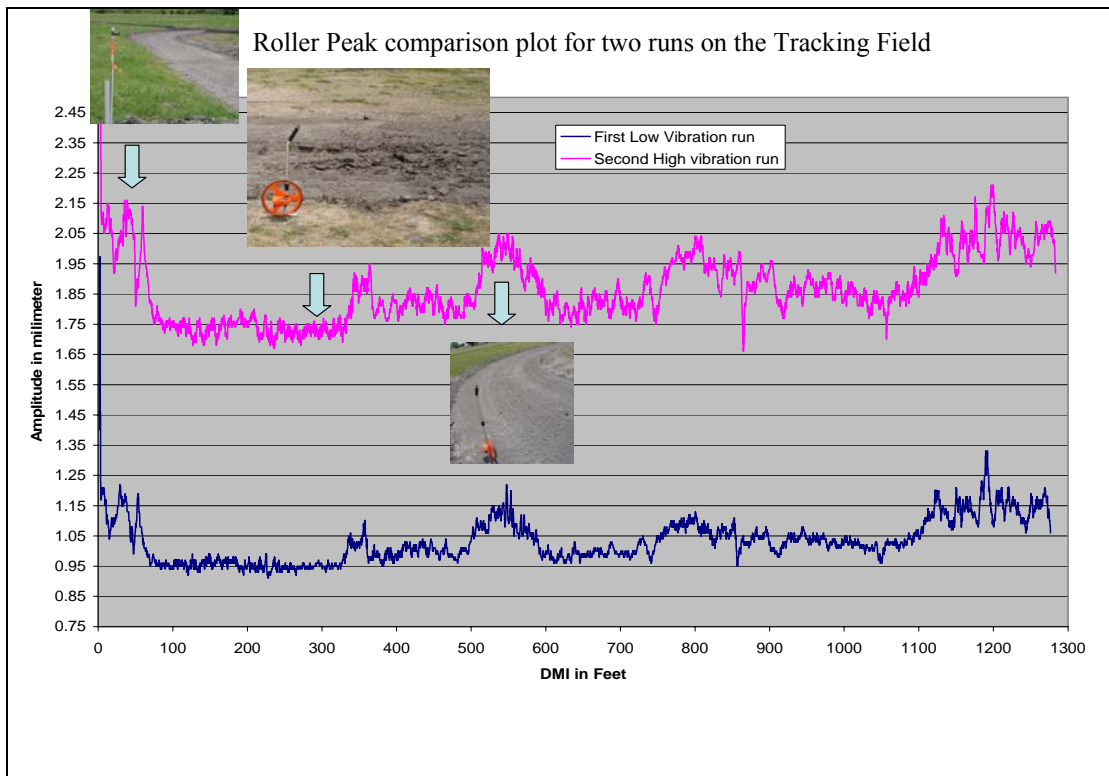


Figure 20. Plot of High and Low Amplitude Displacements Around Running Track.

The software developed in this project was further expanded to summarize the data for user-defined distances for quick review. For this 1300 ft section, researchers decided to summarize the deflection data into 25 ft long sections and to plot these as a histogram of average deflections. The data from this test track are shown in [Figure 21](#).

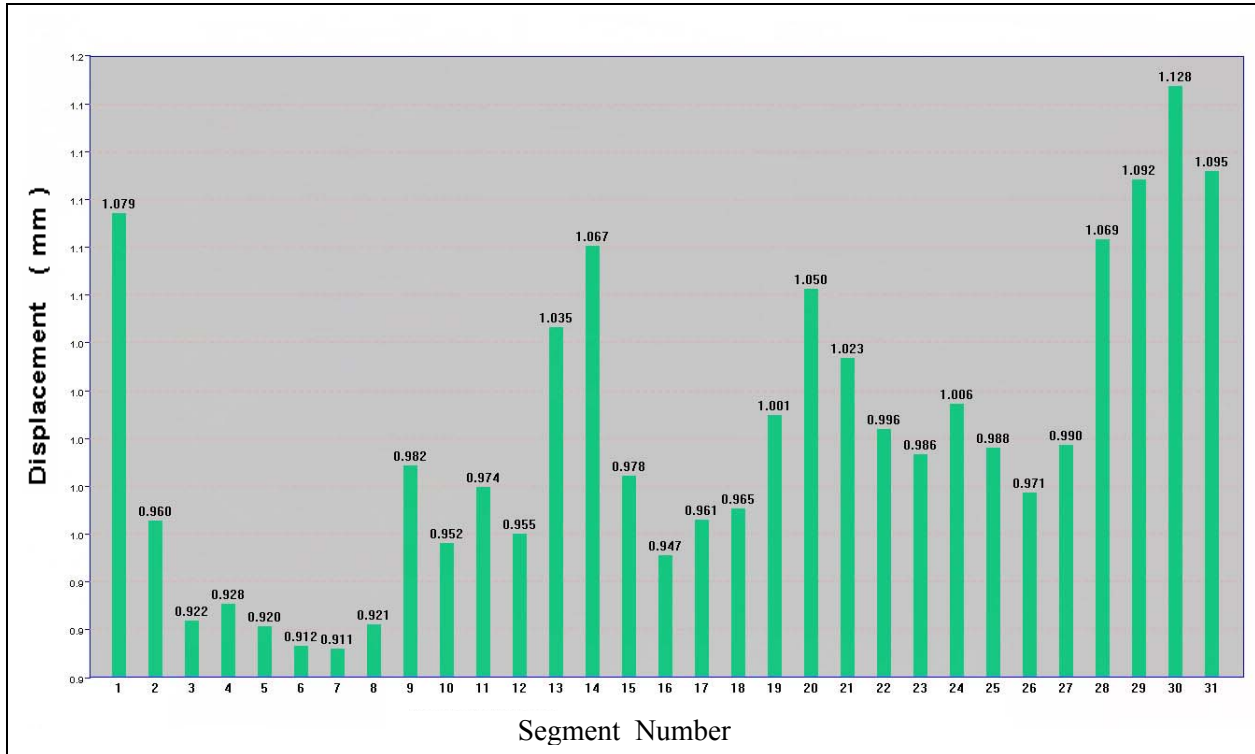


Figure 21. Average Roller Deflections for Each 25 ft Segment of the Test Track.

In practice, a minimum roller deflection could be established for this section, such as the 1.1 mm from the last example. In that case, rolling of the section would continue until all segments of the track had a measured deflection of more than 1.1 mm. While additional compaction will be required for almost all areas, segments 3 through 8 will require the most work.

DEMONSTRATION OF INSTRUMENTED ROLLER ON SH 21 NEAR CALDWELL

Background

A series of tests on SH 21 near Caldwell were undertaken with the intent of determining if the instrument roller could be used to detect areas with poor subgrade support. Secondary tests with DCP, pFWD, and traditional density measuring systems were also performed, and soil samples were taken for laboratory testing. The test site was part of a TxDOT road-widening project conducted by Young Brothers Construction and was located west of the intersection of SH 21 and 60. [Figure 22](#) shows the test area.



Figure 22. Testing of TxDOT Construction Project on SH 21.

The test area was approximately 8 feet wide and extended approximately 1000 feet. The test area was located within a cut section that was to be lime stabilized. The roller movement over the test strip is shown in [Figure 23](#).

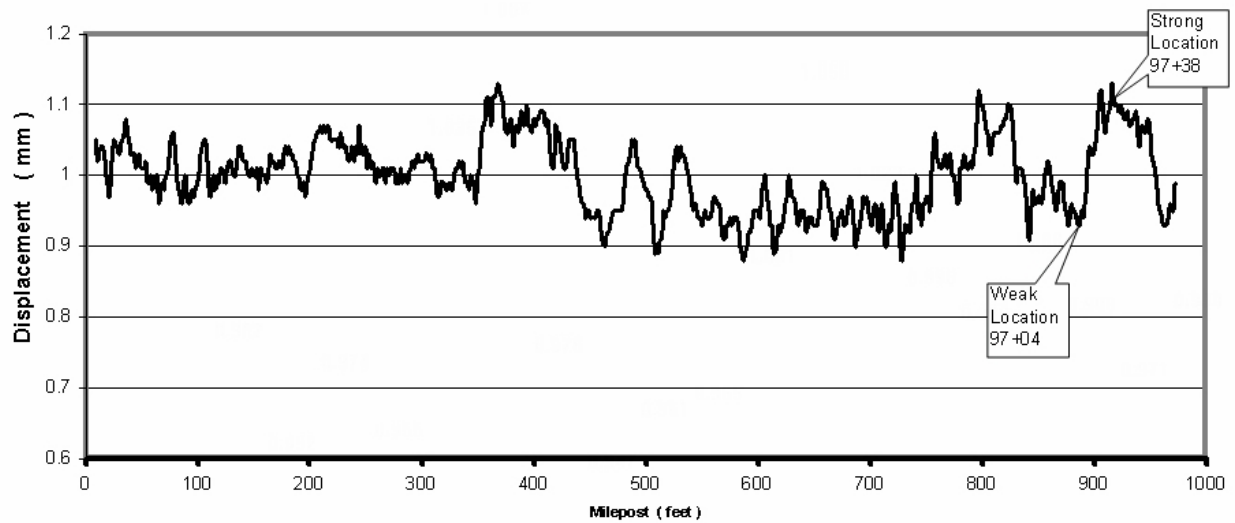


Figure 23. Roller Displacement Along the Length of Test Section.

Based on the results from the previous testing at the Riverside campus a “strong” and a “weak” area were marked for validation testing. These were designated as station 97 + 04 ft which was a “weak” area due to a roller displacement of 0.95 mm and station 97 + 38 ft which was classified as “strong” with a roller displacement of 1.08 mm. Each of the two selected points was tested with the pFWD, DCP, and nuclear gauge. Shelby tube samples were also taken to a depth of 4 ft at each of these locations.

Field Results

At the two locations designated as weak (97 + 04) and strong (97 +38) portable FWD data was collected. At each location two drops of the pFWD were made. The results and computed layer moduli are shown in [Table 3](#). From the DCP data researchers found that this entire area had approximately a 9 inch compacted layer on top of a variable subgrade layer. The data collected by the pFWD and the layer moduli reported by the system are displayed in [Table 3](#). From [Table 3](#), we notice that the two locations’ top layers have nearly the same strength, which is around 5.0 ksi. The bottom layer’s strength at these two locations varies considerably. These variations contribute significantly to the roller’s response.

Table 3. pFWD Data.

| Point | Force (lb) | Pressure (psi) | D1 (mil)* | D2 (mil)* | D3 (mil)* | E1 (ksi) | E2 (ksi) |
|----------|------------|----------------|-----------|-----------|-----------|----------|----------|
| 97+04 d1 | 532 | 10.96 | 9.331 | 2.323 | 1.22 | 5.4 | 5.5 |
| 97+04 d2 | 530 | 10.91 | 9.016 | 2.323 | 1.22 | 5.6 | 5.4 |
| 97+38 d1 | 518 | 10.66 | 8.189 | 0.827 | 0.472 | 5.0 | 14.5 |
| 97+38 d2 | 511 | 10.52 | 8.268 | 0.827 | 0.472 | 5.0 | 14.3 |

*1 mil equals 0.001 inches.

Dynamic Cone Penetrometer data was also collected on the two locations. The results are shown in [Table 4](#). The DCP did a good job of characterizing the site. The upper 9 inches in both cases is similar but in the area designated as weak, the rate of penetration increased markedly with depth. At the weak location below 9 inches, the penetration rate was over 2 inches per blow. In the strong location the penetration rate was similar for the entire top 30 inches.

Table 4. DCP Results for SH 21 Soil Sample Points.

| Station | | Top | Bottom | Thick (in) | Blows | PR (in/blow) | PR (mm/blow) |
|---------|---------|------|--------|------------|-------|--------------|--------------|
| 97+04 | Layer 1 | 0.00 | 8.88 | 8.88 | 11.00 | 0.81 | 20.57 |
| | Layer 2 | 8.88 | 29.31 | 20.44 | 10.00 | 2.04 | 52.12 |
| | | | | | | | |
| Station | | | | | | | |
| 97+38 | Layer 1 | 0.00 | 29.94 | 29.94 | 41.00 | 0.73 | 18.62 |

The data collected by the Nuclear Density Gauge and how the data compares with the measured wet and dry densities and moisture contents is provided in [Table 5](#). The nuclear density gauge did not detect any significant differences between the two locations despite the marked differences in penetration rate.

Table 5. Troxler and Calculated Wet and Dry Densities and Moisture Contents.

| | | Troxler | Troxler | Troxler | Lab Sample | Lab Sample | Lab Sample |
|---------|------------|-------------------|-------------------|----------------------|-------------------|-------------------|----------------------|
| Station | Depth (in) | Wet Density (pcf) | Dry Density (pcf) | Moisture Content (%) | Wet Density (pcf) | Dry Density (pcf) | Moisture Content (%) |
| 97+04 | 6 | 131.2 | 111.5 | 17.68 | 132.8 | 109.29 | 17.71 |
| | 12 | 132.8 | 113.1 | 17.48 | | | |
| 97+38 | 6 | 131.6 | 112 | 17.55 | 133.8 | 110.87 | 17.15 |
| | 12 | 132.4 | 112.9 | 17.31 | | | |

Laboratory Results

A laboratory testing program was developed to determine the insitu characteristics of the subgrade soil on the SH 21 test site. Shelby tube samples of approximately 2.8 inches in diameter were taken from within the test section. Four borings were advanced to a depth of 4 feet at each of the two locations. Tests were conducted to determine the density (wet and dry), Atterburg limits, and resilient modulus. The samples were stored in insulated coolers in TTI’s 100 percent humidity room in order to minimize moisture change.

It was not possible to obtain 100 percent recovery during Shelby tube sampling. As such, it is possible that some of the tested samples contained soil from both the top and the bottom layer. Future sampling protocols will attempt to address this limitation so that the number of samples containing soil from only one layer is maximized.

A brief description of each test, and what data is obtained from each test, is provided in the [following section](#):

Density

Both the wet and dry densities were calculated using the samples prepared for the resilient modulus tests. The height and circumference of each sample was measured in three places, and the average value of each was determined for use in calculating the volume of the sample. The sample was weighed prior to testing. The moisture content of the sample was determined by taking the average of three moisture tests conducted on trimmings from the soil adjacent to the top and bottom of the sample. An overall moisture content was determined after final testing by drying the entire sample.

Resilient Modulus

The resilient modulus is based on the stress/strain behavior of a material that is repeatedly loaded and unloaded under varying confining pressures. The testing sequence used on the 2.8 inch diameter Shelby tube samples obtained from SH 21 is provided below in [Table 6](#).

Table 6. Resilient Modulus Testing Protocol.

| Sequence | Confining Pressure (psi) | Confining Force (#) (pounds) | Contact Stress (psi) | Contact Force (pounds) | Cyclic Stress (psi) | Cyclic Force (pounds) | Maximum Stress (psi) | Maximum Force (pounds) | Reps |
|----------|--------------------------|------------------------------|----------------------|------------------------|---------------------|-----------------------|----------------------|------------------------|------|
| Precon. | 4 | 26.6 | 0.8 | 5.3 | 1 | 6.7 | 1.8 | 12.0 | 100 |
| 1 | 8 | 53.2 | 1.6 | 10.6 | 4 | 26.6 | 5.6 | 37.2 | 100 |
| 2 | 6 | 39.9 | 1.2 | 8.0 | 4 | 26.6 | 5.2 | 34.6 | 100 |
| 3 | 4 | 26.6 | 0.8 | 5.3 | 4 | 26.6 | 4.8 | 31.9 | 100 |
| 4 | 2 | 13.3 | 0.4 | 2.7 | 4 | 26.6 | 4.4 | 29.3 | 100 |
| 5 | 8 | 53.2 | 1.6 | 10.6 | 7 | 46.6 | 8.6 | 57.2 | 100 |
| 6 | 6 | 39.9 | 1.2 | 8.0 | 7 | 46.6 | 8.2 | 54.5 | 100 |
| 7 | 4 | 26.6 | 0.8 | 5.3 | 7 | 46.6 | 7.8 | 51.9 | 100 |
| 8 | 2 | 13.3 | 0.4 | 2.7 | 7 | 46.6 | 7.4 | 49.2 | 100 |
| 9 | 8 | 53.2 | 1.6 | 10.6 | 10 | 66.5 | 11.6 | 77.2 | 100 |
| 10 | 6 | 39.9 | 1.2 | 8.0 | 10 | 66.5 | 11.2 | 74.5 | 100 |
| 11 | 4 | 26.6 | 0.8 | 5.3 | 10 | 66.5 | 10.8 | 71.8 | 100 |
| 12 | 2 | 13.3 | 0.4 | 2.7 | 10 | 66.5 | 10.4 | 69.2 | 100 |
| 13 | 8 | 53.2 | 1.6 | 10.6 | 14 | 93.1 | 15.6 | 103.8 | 100 |
| 14 | 6 | 39.9 | 1.2 | 8.0 | 14 | 93.1 | 15.2 | 101.1 | 100 |
| 15 | 4 | 26.6 | 0.8 | 5.3 | 14 | 93.1 | 14.8 | 98.4 | 100 |
| 16 | 2 | 13.3 | 0.4 | 2.7 | 14 | 93.1 | 14.4 | 95.8 | 100 |

At each one of the test conditions the resilient modulus of the soil is calculated. This result is then fit to a non-linear resilient modulus regression model as shown below. The resilient modulus is calculated by the [following equation](#), which is being adopted in the NCHRP 1-37A project (2002 design guide):

$$M_r = k_1 P_a \left(\frac{\theta}{P_a} \right)^{k_2} \left(\frac{\tau_{oct}}{P_a} + 1 \right)^{k_3} \quad (1)$$

Where:

$$k_1, k_2 \geq 0,$$

$$k_3 \leq 0,$$

M_R = resilient modulus,

$$\tau_{\text{oct}} = \text{octahedral shear stress} = \frac{1}{3} \sqrt{(\sigma_1 - \sigma_2)^2 + (\sigma_1 - \sigma_3)^2 + (\sigma_2 - \sigma_3)^2} ,$$

θ = bulk stress = $\sigma_1 + \sigma_2 + \sigma_3$,

$\sigma_1, \sigma_2, \sigma_3$ = principal stresses,

k_i = regression constants, and

P_a = atmospheric pressure.

Terms $k_1, k_2,$ and k_3 are material properties, which are computed from regression analysis. Once the least squared regression components are computed, the measured versus computed resilient modulus is graphed as shown in [Figure 24](#).

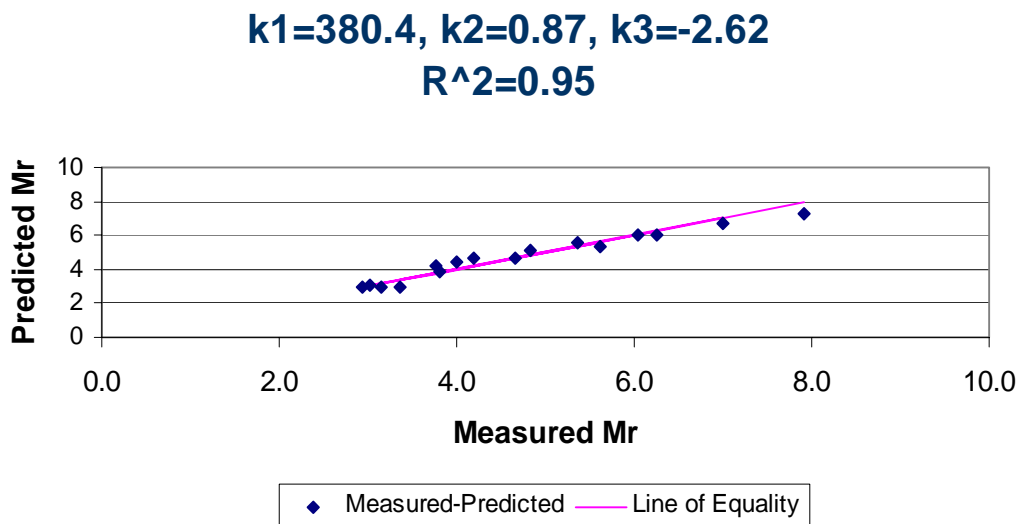


Figure 24. Typical Plots of Measured versus Computed Resilient Modulus.

The resilient modulus for design is determined based on selecting a stress condition which will be appropriate for the stresses which will be anticipated under traffic loading. For this project researchers assumed a deviator stress of 15 psi and a confining stress of 5 psi. For the weak and strong sections under consideration, soils from the 2 to 4 feet depth were tested, and the results are shown in [Table 7](#). This resulted in the design moduli (M_R) shown in the last column of [Table 7](#).

Table 7. Resilient Moduli.

| Station, Direction, and Depth (ft) | k1 | k2 | k3 | R sq | Mr (ksi) |
|------------------------------------|------|-------|------|------|----------|
| 97+38, East, 2 to 4 | 4941 | 0.0 | 0.38 | 0.94 | 62 |
| 97+38, South, 2 to 4 | 4960 | -0.02 | 0.61 | 0.98 | 56 |
| 97+04, South, 2 to 4 | 1900 | 0.0 | 2.46 | 1.0 | 10.6 |
| 97+04, West, 2 to 4 | 1950 | 0.0 | 2.06 | 1.0 | 12.7 |

As expected, the moduli for Station 97+38 were substantially higher than those for 97+04, however the values seem to be too high. As shown, the samples were retested, and the second set of values was similar to the first set. It is possible that the deviator stress was not large enough to elicit an appropriate response from the material. This potential issue will be addressed in future testing. However, as predicted by the roller deflections the soils at 97+38 are substantially stiffer than the soils at 97 + 04.

The Atterberg limits for the two locations are shown in [Table 8](#).

Table 8. Atterberg Limits.

| Location, Direction, Depth (ft) | LL | PL | PI |
|---------------------------------|----|----|----|
| Station 97+38, West, 0 to 2 | 44 | 14 | 30 |
| Station 97+38, West, 2 to 4 | 49 | 16 | 33 |
| Station 97+04, East, 0 to 2 | 38 | 13 | 25 |
| Station 97+04, East, 2 to 4 | 40 | 14 | 26 |

Evaluation of Results

The premise of this testing was that the roller displacements from the two locations were indicative of the strength of the subgrade support. To evaluate this premise, direct comparison of the location with other test measurements was preformed.

The roller displacements compared with the other measurements are presented in [Tables 9-12](#). A comparison is made of the rankings made with the roller as compared to the ranking from the other devices.

Table 9. Roller Displacement versus DCP Penetration Rate (> 9 inches deep).

| Test Section | Roller Displacement (mm) and rank (high to low) | DCP Penetration Rate (in/blow) and rank (high to low)* |
|--------------|---|--|
| 97+04 | 0.95 (2) | 2.04 (2) |
| 97+38 | 1.08 (1) | 0.73 (1) |

*lower penetration rate denotes stronger material

Table 10. Roller Displacement versus Lab Resilient Modulus (2-4 feet deep).

| Test Section | Roller Displacement (mm) and rank (high to low) | Lab Resilient Modulus (ksi) and rank (high to low) |
|--------------|---|--|
| 97+04 | 0.95 (2) | 11.5 (2) |
| 97+38 | 1.08 (1) | 58 (1) |

Table 11. Roller Displacement versus Pocket Penetrometer Su.

| Test Section | Roller Displacement (mm) and rank (high to low) | Pocket Penetrometer Su (psi) and rank (high to low) |
|--------------|---|---|
| 97+04 | 0.95 (2) | 2,562 (2) |
| 97+38 | 1.08 (1) | 3,812 (1) |

Table 12. Roller Displacement with Nuclear Density Readings.

| Test Section | Roller Displacement (mm) and rank (high to low) | Nuclear Density Gauge | | Laboratory Measured | |
|--------------|---|--|--|--|--|
| | | Wet Density (pcf) and rank (high to low) | Dry Density (pcf) and rank (high to low) | Wet Density (pcf) and rank (high to low) | Dry Density (pcf) and rank (high to low) |
| 97+04 | 0.95 (2) | 132.0 (tie) | 112.3 (2) | 132.8 (2) | 109.3 (2) |
| 97+38 | 1.08 (1) | 132.0 (tie) | 112.5 (1) | 133.8 (1) | 110.8 (1) |

The most interesting feature in Tables 9-12 was that the nuclear density gauge did a relatively poor job at differentiating between the weak and strong locations. Even when the probe was placed at a depth of 12 inches, the gauge did not find any difference between the two sites even when the DCP recorded a large reduction in layer strength at a depth of 9 inches below the surface. However, the DCP did indicate that the two locations were similar in stiffness throughout the top 9 inches. All the other devices found these sites to be significantly different in terms of overall support. This difference is explained by the fact that the nuclear density gauge is testing the upper layers in the structure whereas the instrumented roller is testing the complete structural integrity of the entire section.

SUMMARY OF FINDINGS FROM INSTRUMENTED ROLLER

The prototype roller developed on this project was successfully tested in these pilot investigations. The roller responses were found to be repeatable and related to the overall support of the subgrade. The instrumented roller can be used to locate weak areas in the foundation layer. However, the roller responses were not related to the density or stiffness of the upper layer so there was not a good correlation with nuclear density readings. Further testing is required with this roller. This testing will involve additional testing of TxDOT projects where data can be collected on top of raw subgrades, stabilized subgrades, and flexible bases. As performed on SH 21, validation tests will need to be performed primarily with the DCP.

CHAPTER 4

DEVELOPMENT OF A NEW INFRARED IMAGING SYSTEM FOR HOT-MIX ASPHALT OVERLAYS

SUMMARY

Project 0-4126 (Sebesta and Scullion 2002), along with several studies performed by other agencies (Read 1996; Stroup-Gardiner and Brown 2000; and Willoughby et al. 2001), lent strong support to the notion that infrared imaging could serve a useful purpose for inspecting paving operations for uniformity and segregation. Substantial research indicates that temperature differentials in excess of 25 °F indicate potential segregation in the hot-mix mat. All the previous studies used infrared cameras for the inspection tool. Because of deficiencies with this technique, TTI researchers undertook development of an infrared sensor bar to use in place of the camera. This chapter describes the development of the Pave-IR system, which enables personnel to efficiently collect and summarize infrared temperature data from a paving project to evaluate the project for uniformity and segregation.

DESIRED FEATURES OF INFRARED SYSTEM

Figure 25 shows the basic design idea for the infrared sensor bar. The TTI team set forth several key features to incorporate into the infrared sensor bar system. Some features are specific to the hardware, while some are handled by software features. The primary functions the research team desired in the system include:

- Hardware Features:
 - Rapid setup time
 - Flexibility to survey projects of varying paving widths
 - Ability to include a distance encoder
 - Ability to adjust height of infrared sensors
 - Robust
- Software Features:
 - Ability to collect data in a distance mode
 - Real-time color display of data

- Ability to quickly identify when temperatures in a transverse scan stray from acceptable limits
- Ability to quickly evaluate the overall uniformity of a project as data are collected
- Ability to quickly summarize results from an entire project

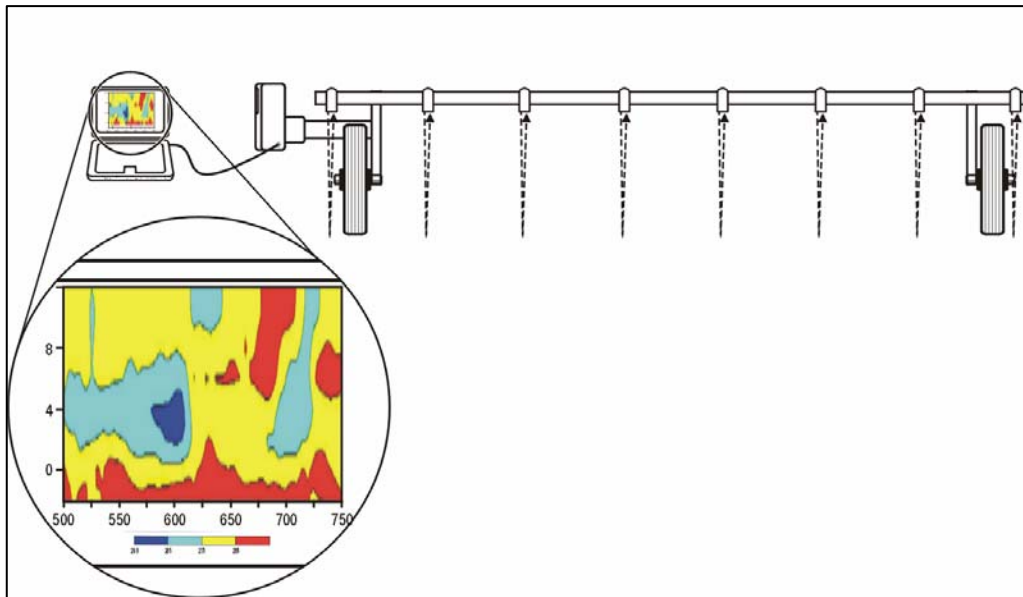


Figure 25. Design Idea for Infrared Sensor Bar (Sebesta and Scullion 2002).

The initial development of prototypes is described in TTI Report 0-4577-2 (Sebesta et al. 2005). The initial unit was a push behind unit, where the operator walks behind the paver. Currently, a total of 10 paving projects have been tested with the basic temperature bar setup. The new generation system, called Pave-IR, attaches directly to a paver and to date has been utilized on two paving projects. Details of the new system are described below.

OVERVIEW OF THE CURRENT PAVE-IR SYSTEM

To overcome the problems noted with the infrared cameras, a team at the Texas Transportation Institute set out to bring the infrared temperature bar concept to fruition. Primary design features, problems encountered, and development of the first two generation devices are described in TTI Report 0-4577-2 (Sebesta et al. 2005). Table 13 summarizes key hardware specifications of the current Pave-IR.

Table 13. Key Pave-IR Hardware Specifications.

| | |
|--|-----------------------|
| Number of infrared sensors | 10 |
| Typical sensor spacing | 13 inches |
| Mat analysis width | 10 to 12 feet |
| Typical sensor working height | 3 feet |
| Sensor spectral response range | 8 to 14 μm |
| Sensor distance:spot ratio | 10:1 |
| Sensor temperature measurement range | -40 to 1112 °F |
| Sensor ambient operating temperature range | 32 to 185 °F |

The current Pave-IR system uses two temperature bars attached directly to the paver. Each bar contains five infrared sensors. When compared to previous operator-propelled prototypes, this two-bar setup allows for easier transport, improved setup time, and improved safety of operators by eliminating the need for personnel to push the bar. This setup also ensures constant distance of the temperature bars behind the screed. In addition to the new two-piece temperature bar, the current Pave-IR system uses a master control cable that links the temperature bars to a master control box. This new cable significantly reduces the quantity of exposed wiring, and the control box contains all the necessary signal conditioners and the data transfer junction for connection to the computer.

Figure 26 shows the current Pave-IR system in use on a paving project. The two cables coming from the temperature bars at the middle of the paver merge into one cable before connecting to the master control box.



Figure 26. TTI's Current Pave-IR System Collecting Project Data.

CLOSER DETAILS OF PAVE-IR SYSTEM COMPONENTS

While the basic idea of Pave-IR simply centers on infrared sensors above a pavement mat, the finer details make the system near ready for full implementation. TTI has developed a method for system calibration, and hardware which is rugged in the field, simple to set up, and easy to maintain. An accompanying software package created by TTI is simple to operate and handles all functions of Pave-IR ranging from calibration to real-time data display to post-processing analysis.

System Calibration

To ensure accuracy of the infrared sensors, Pave-IR software includes a module for calibration of the infrared sensors. The calibration is performed in the lab with a blackbody source with an accuracy of $\pm 0.9\text{ }^{\circ}\text{F} \pm 0.25$ percent of reading and a stability of $\pm 0.2\text{ }^{\circ}\text{F}$. [Figure 27](#) illustrates the basic calibration setup.



Figure 27. Infrared Sensor Installed in Blackbody Source for Calibration.

System Hardware

The Master Control Box

Figure 28 shows the master control box previously described. This box weighs approximately 18 lb and measures approximately 15 x 11 x 10 inches. The control box helps ensure easy setup and transportability of many required Pave-IR components while also providing the components protection from damage. This box also contains an inverter to provide 120 VAC power to eliminate dependency on laptop batteries for running the computer. The paver battery provides power to the master control box to run the system. If in need of servicing, the box can be disassembled by simple removal of sheet metal screws. This control box replaced the operator-propelled carts used in previous systems.



Figure 28. Master Control Box for Pave-IR.

The Temperature Bars

The current Pave-IR temperature bars contain the infrared sensors already mounted and pre-wired for easy connection to the master control box. Each bar opens along a hinged joint for access to the sensors and internal wiring. When closed and secured shut, the bars provide protection to the sensors and wiring. Slots in the bars allow adjustment of sensor spacing to measure paving widths ranging from 10 to 12 ft. [Figure 29](#) shows the sensor side and the internal side of a temperature bar.



Figure 29. Sensor Side and Internal Sides of Temperature Bar.

Software

Pave-IR software completes the Pave-IR system. This software allows for calibration of the sensors, calibration of the DMI, collection of transverse scans at user-defined distances (typically set at every 2 inches), real-time data display, real-time analysis of whether temperatures in a scan fall within user-defined limits, real-time display of a histogram of measured temperatures at user-defined intervals (typically set at every 100 ft), post-processing data playback, and post-processing display of a histogram of measured temperatures for the entire project. [Chapter 5](#) of this report illustrates some of the features of Pave-IR software by illustrating results from several field projects.

CHAPTER 5

EXAMPLE DATA FROM PAVE-IR

SUMMARY

This chapter presents example data from Pave-IR from three separate field projects and illustrates the application of Pave-IR. The Pave-IR system can be used to evaluate mat placement variability and then later used to verify the effectiveness of any corrective action taken. Without Pave-IR, the variability occurring on these paving projects likely would not have been detected.

RESULTS FROM TYPE D HMA IN PARIS DISTRICT

On this Type D mix placed in January 2005, a thermal survey revealed significant temperature differentials along the longitudinal profile. This project utilized end-dump trucks into a Material Transfers Device (MTD). Based on observations at the project site and discussions with project personnel, numerous recommendations were made regarding the project involving everything from plant operations through rolling patterns. Based upon the survey, TxDOT met with the contractor and worked to improve the quality and uniformity of the project through better control at the plant, utilization of a different model MTD, and altered rolling patterns. With modified operational procedures, the project resumed in April 2005. Collected data show the operational changes significantly improved mat placement uniformity. Figures 30 and 31 contrast the resultant thermal profiles from the initial to the modified operation. Figures 32 and 33 illustrate how the changes in operations significantly tightened the measured placement temperature distribution. With the initial operation, approximately 95 percent of measured temperatures fell within a 90 °F window. With the new operation based upon the recommendations from the thermal survey, approximately 95 percent of measured temperatures fell within a 40 °F window. Based upon recommendations from the initial project survey with Pave-IR, the modified operation reduced the range of mat placement temperatures by over 50 percent. Without Pave-IR, the extent of variability in the initial paving operation likely would not have been discovered.

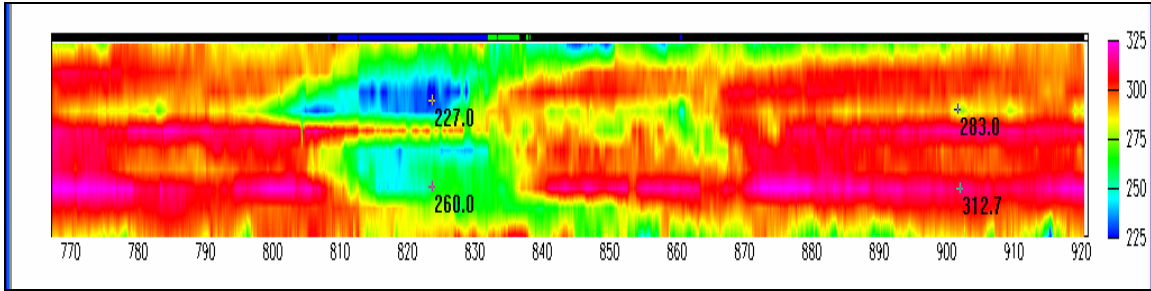


Figure 30. Example Thermal Profile from Initial Paving Operation on US 82.

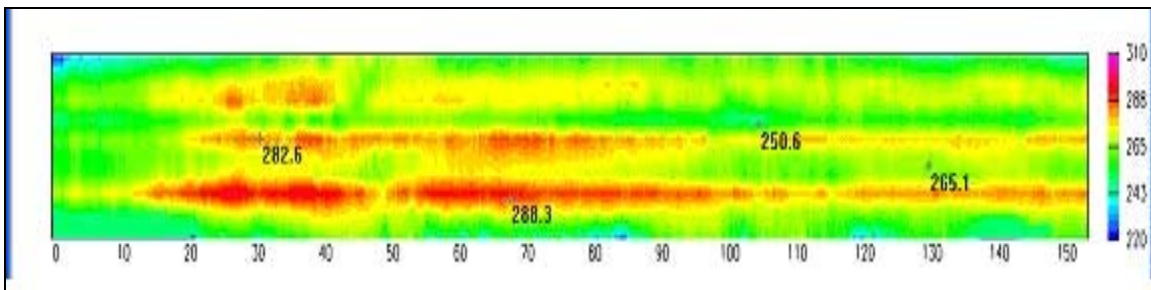


Figure 31. Example Thermal Profile from Modified Paving Operation on US 82.

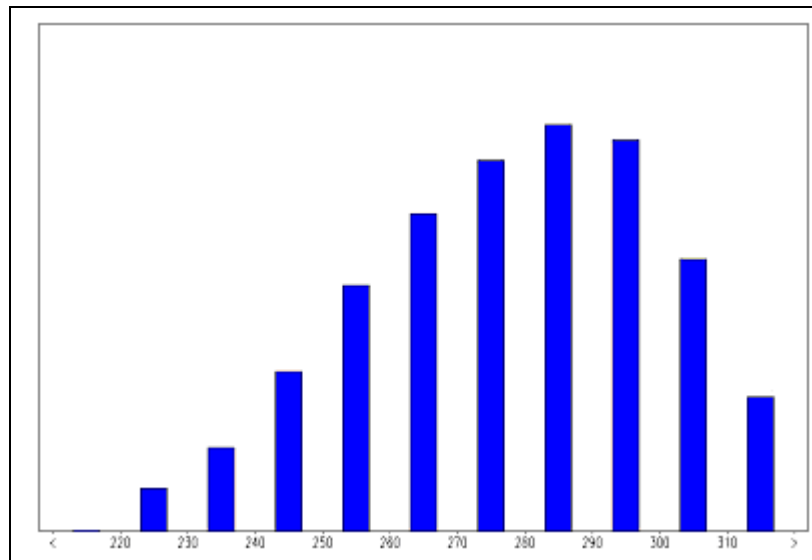


Figure 32. Histogram of Measured Mat Placement Temperatures from Initial Paving Operation on US 82.

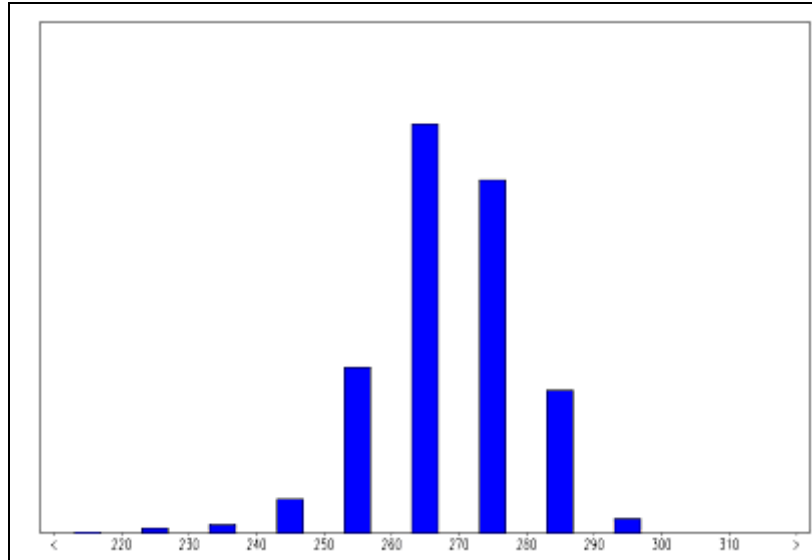


Figure 33. Histogram of Measured Mat Placement Temperatures from Modified Paving Operation on US 82.

TYPE D HMA IN FORT WORTH DISTRICT

On this paving project in July 2005, the supply of trucks was sporadic, resulting in frequent paver stops. At times the wait between trucks approached 20 minutes. Once the paving train resumed progress, Pave-IR showed transverse locations of excessively hot spots, illustrated in Figure 34. Investigation into the cause of these hot spots revealed that, with the paver idle and waiting for the next truck, the contractor continuously ran the burners. After discovering this problem, the contractor ceased the continual operation of the burners when the paver was stationary.

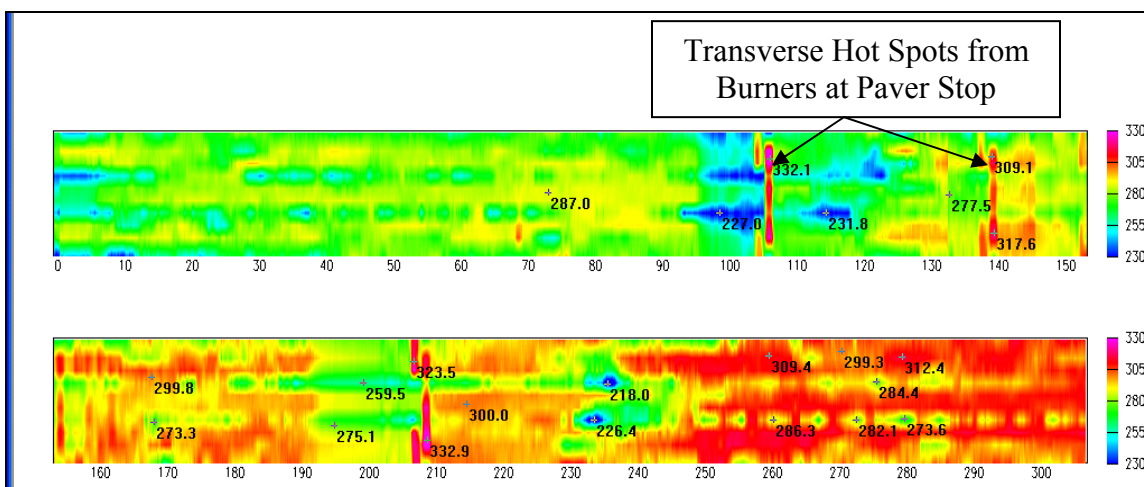


Figure 34. Hot Spots from Burner Operation on Idle Paver.

TYPE D HMA ON US 90 IN HOUSTON DISTRICT

Figure 35 shows the location of this project on US 90, placed in August 2005. Pave-IR data revealed quite good uniformity in mat placement temperatures, although occasionally within a few truckloads the mean placement temperature spiked substantially. Figure 36 presents an excerpt from one such location, it illustrates an example of the transition of mean placement temperatures between truckloads. The mean placement temperature for this project was between 270 and 280 degrees, however at the location shown in Figure 36 the temperature was over 330 degrees. From the distance scale it appears that three truck loads of hot mix were substantially higher than the rest of the project. Also Pave-IR showed a location of cold mix where the paver had stopped. Figure 37 shows this location, which occurred at 4770 feet into the run.

On this project, the Pave-IR system worked quite well, collecting over 2 miles of continual data. The main problem noted was that the computer got too hot; investigation into reliability of the computer system used to control Pave-IR needs to be pursued to improve the field ruggedness of the system.

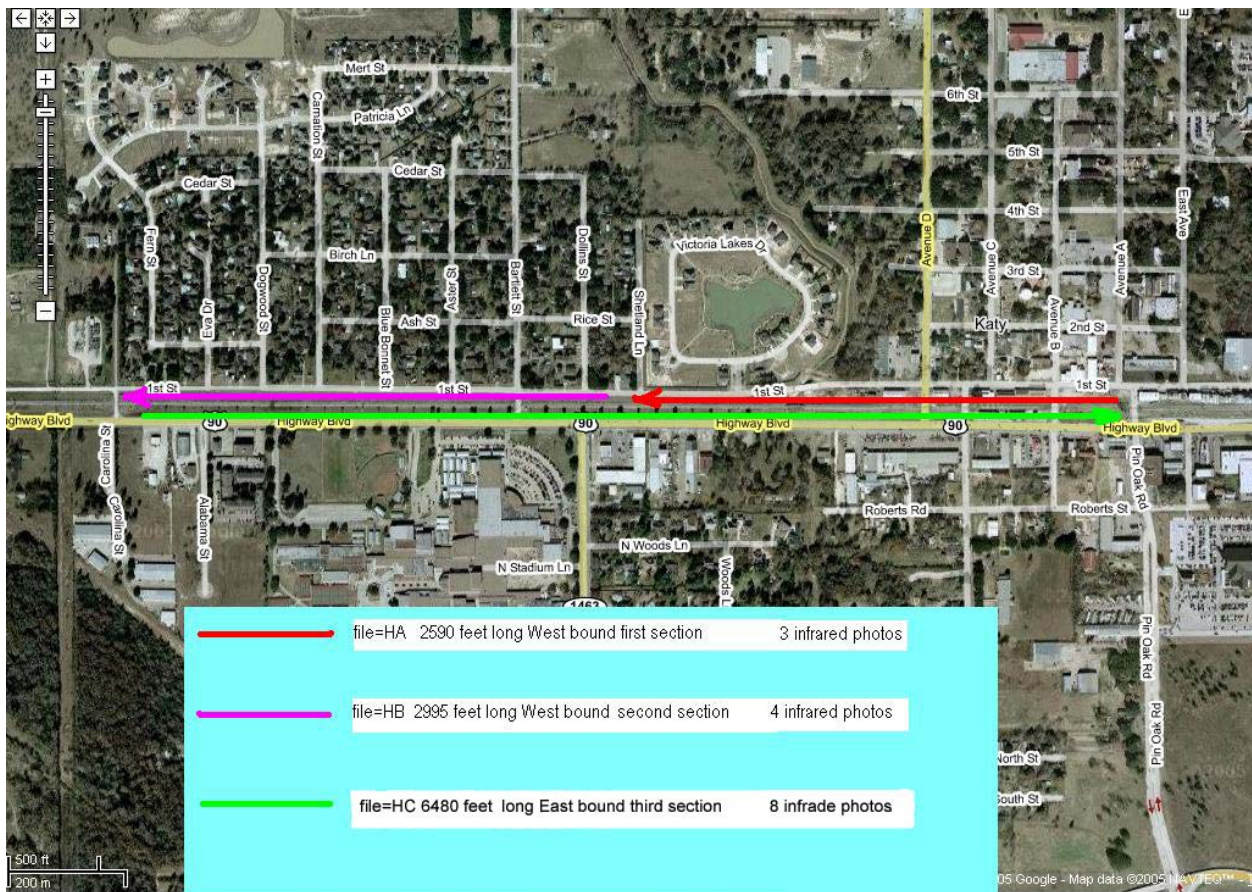


Figure 35. Location of Pave-IR Testing on US 90 in August 2005.

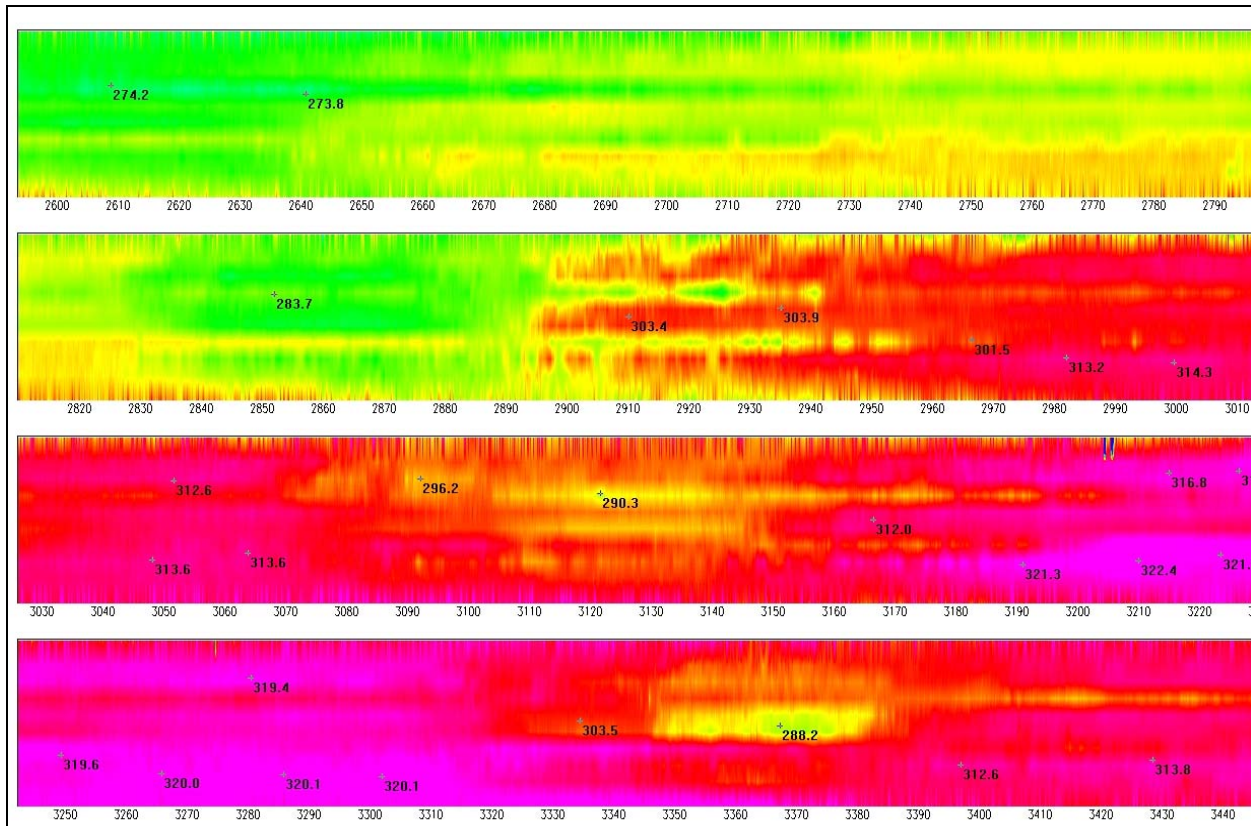


Figure 36. Increase in Mean Placement Temperatures on US 90.

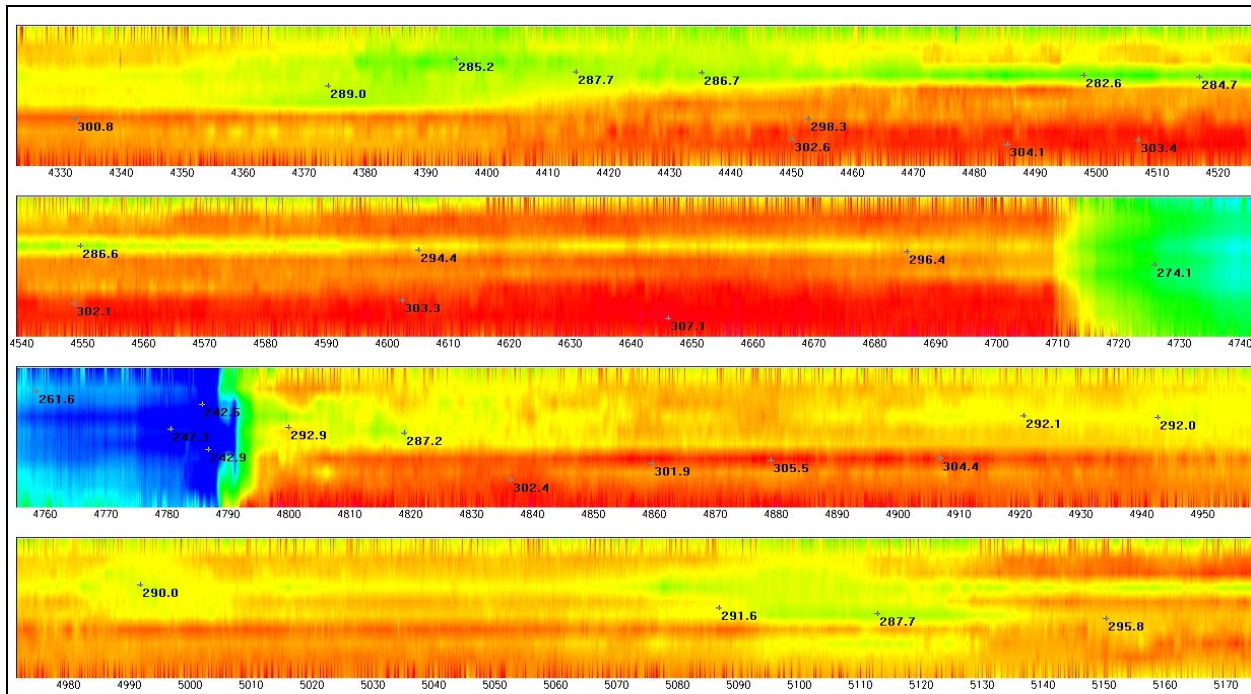


Figure 37. Location of Paver Stop on US 90 Eastbound.

CHAPTER 6

CONCLUSIONS AND RECOMMENDATIONS

Developing and implementing new technologies to assist in monitoring the quality of new pavements is a high priority item. It has become even more critical in recent times because of the heavy project load and because TxDOT inspectors are often stretched with demanding work loads and round the clock construction. In addition, the move to paving at night in many urban districts makes it even more challenging to check the uniformity of new asphalt surfaces. The recent development of new design-build contracts has also focused TxDOT's senior management on new ideas for measuring quality. The concepts described in this report appear ideal to address many of these QC/QA issues.

The two 100 percent coverage systems developed by TTI during this project show great potential to be refined into viable systems. The infrared system is ready for full-scale evaluation and for eventual consideration for inclusion in draft specifications. A possible draft specification for IR testing is attached in the [Appendix](#) to this report. The main issue in the new draft specification is that the infrared bar can detect cold spots in the mat, and these areas should be checked with traditional density gauges after compaction. This concept is already in the specifications used by Washington State DOT.

The instrumented roller developed on this project was successfully tested in pilot investigations. The roller responses were found to be repeatable and related to the overall support of the subgrade. The instrumented roller can be used to locate weak areas in the foundation layer. However, the roller responses were not related to the density or stiffness of the upper layer so there was not a good correlation with nuclear density readings. Further testing and development is required with this roller. This will involve additional testing on TxDOT projects where data can be collected on top of raw subgrades, stabilized subgrades, and flexible bases. As performed on SH 21 validation tests will need to be performed.

Among the items that need to be addressed in future instrumented roller testing, and possible methods to achieve the objectives, are the following:

1. Harden and simplify the system so that it can be used by construction personnel in the field.

- a. Research commercially available components such as accelerometers, data acquisition systems, and DMIs that are reliable and weatherproof.
 - b. Provide a color-coded display in the roller operator's cab that will provide for easy identification of weak areas.
 - c. Develop an operator's manual that explains installation and how to interpret the results.
2. Determine the affect of layering on the amount of displacement measured by the accelerometer.
 - a. Perform DCP analysis at future test sites prior to the roller system being used to determine layer characteristics.
 - b. Conduct tests on stabilized bases and flexible bases.
3. Determine the depth to which use of the vibratory roller can cause sufficient improvement of the soil properties to meet the requirements outlined in the specifications.
 - a. Perform pFWD, DCP, and possibly FWD analysis prior to and after the use of the roller system to determine to what depth improvement occurred.
4. Identify the effect of weather particularly rainfall and extended periods of dry weather on roller response.
5. Most importantly, determine how specifications can be developed to be incorporated in any project. The roller concept is new so careful consideration should be given on how to do this. This will require:
 - a. A review of foreign specifications, particularly Germany (where at the onset of specification development the roller was compared with plate bearing tests).
 - b. A comparison with pavement design requirements. Every structural design in Texas has an assigned subgrade modulus value typically between 4 and 20 ksi. This value being from FWD testing on the completed pavement structure. To compare the two measurements it will be necessary to do testing during construction with the instrumented roller, and check the resulting subgrade stiffness after completion with the FWD.
 - c. Investigate how the subgrade modulus of a pavement structure changes with time and determine how this is related to the roller displacements measured during

construction. It has often been said that the Texas subgrades require at least 12 to 18 months to achieve a moisture equilibrium and equilibrium subgrade modulus. These items will be addressed under a new TxDOT implementation project which will be initiated in September of 2005.

In shadow testing on future projects TxDOT should give serious consideration for comparing (and merging) these two new technologies with existing equipment such as nuclear density and FWD testing. The uniformity of support is the major design criteria on large construction projects in Europe, especially Germany. In the European countries, the pavement designs used are standard from catalogues of designs, where the major engineering design work performed is in providing a permanent uniform support layer. In many projects instrumented rollers are used to check this uniformity. These design and testing concepts would be ideal to be incorporated into TxDOT's future perpetual pavement construction or even to test the support layers under the new concrete toll roads being constructed in central Texas. Consideration should be given to shadow testing the following concepts on a major construction project in Texas:

- a) Testing subgrade uniformity with an instrumented roller (with secondary DCP, seismic and laboratory modulus testing to set design standard and target roller movement levels).
- b) Testing uniformity of lime-stabilized layers with an instrumented roller (with the same secondary measurements as described above).
- c) Testing the uniformity of flexible bases with an instrumented roller and falling weight deflectometer.
- d) Quality control testing of new asphalt surfaces with the infrared bar, evaluating the specifications attached to this report (secondary testing with density gauges and coring in suspected defect locations).
- e) Quality assurance testing of new asphalt surfaces with the ground penetrating radar system which can check for mat thickness, surface segregation, compaction problems with depth and joint density (secondary testing with nuclear density gauges and field cores for validation).

REFERENCES

1. Sebesta, S., and T. Scullion. *Using Infrared Imaging and Ground-Penetrating Radar to Detect Segregation in Hot-Mix Overlays*. Report 0-4126-1, Texas Transportation Institute, May 2002.
2. Read, S. *Construction Related Temperature Differential Damage in Asphalt Concrete Pavements*, University of Washington, 1996.
3. Stroup-Gardiner, M., and E.R. Brown. *NCHRP Report 441: Segregation in Hot-Mix Asphalt Pavements*. Transportation Research Board, National Research Council, Washington, D.C., 2000.
4. Willoughby, K., S.A. Read, J.P. Mahoney, S.T. Muench, L.M. Pierce, T.R. Thompson, J.S. Uhlmeier, R. Moore, and K.W. Anderson. *Construction-Related Asphalt Concrete Pavement Temperature Differentials and the Corresponding Density Differentials*. Report WA-RD 476.1. Washington Department of Transportation, July 2001.
5. Sebesta, S., T. Scullion, W. Liu, and C. Estakhri. *Field Evaluation of New Technologies for Quality Control*. TTI Report 0-4774-1, Texas Transportation Institute, September 2004.
6. Forssblad, L. *Roller Mounted Compaction Meters – Principles Field Tests and Practical Experiences*. Proc. of the XIX Ohio River Valley Soil Seminar, Lexington, Kentucky, 1988.
7. Webster, B and R. Grau. *Development of the Dual Mass Dynamic Cone Penetrometer for Subgrade Testing*. US Army COE Report 88-231, Vicksburg, Mississippi, 1988.
8. Lui, W. and T. Scullion. *MODULUS 6 for Windows: Users Manual*. TTI Report 0-1869-3, Texas Transportation Institute, October 2001.
9. Sebesta, S., F. Wang, T. Scullion, and W. Liu. *New Infrared and Radar Systems for Detecting Segregation in Hot-Mix Asphalt Overlays*. Report 0-4577-2, Texas Transportation Institute, February 2005.

APPENDIX

DRAFT SPECIFICATION FOR INFRARED TESTING

The methodology of using thermal imaging to detect localized thermal segregation is already in the Washington DOT specification <http://www.wsdot.wa.gov/fasc/engineeringpublications/manuals/2006ss.htm>, under Division 5, section 5-04-3(10)B, in the section on low cyclic density). The pay reduction issue and approach defined below are similar to the Washington DOT specification. In Washington an infrared camera is used to detect the low temperature areas. In the proposed Texas specification the infrared bar developed in this project will be used.

DETECTING SEGREGATION WITH PAVE-IR

Section 1. Overview

This method uses the Pave-IR thermal imaging system to detect potentially segregated areas on a newly placed, uncompacted, hot-mix asphalt overlay. The thermal profile is acquired with an infrared temperature bar controlled by a laptop computer with appropriate software. This method requires the user to possess a working knowledge of the Pave-IR data collection equipment and Pave-IR operating software.

This testing is performed on a per-lot basis. Once the cold spots are identified in the IR data these spots are tested with traditional density testing. Four spots are selected for coring, and lab densities are measured. If three of the tested area have less than 89% density then the contractor would receive a 15% pay reduction for that lot.

Section 2. Definitions

Thermal segregation is defined as an area with temperature differentials greater than 25 °F.

Section 3. Apparatus

- Infrared temperature bar capable of imaging at least a 12 ft wide mat and including a minimum of 10 sensors, each with a distance:spot ratio of 2:1, a spectral response of 8 to 14 μm , a measurement temperature range that includes -40 to 1112 °F, and capable of operating in ambient temperatures ranging from 32 to 185 °F.
- Laptop computer with Pave-IR operating software.

Section 4. Procedure

| Locating Potential Segregation with Pave-IR | |
|--|---|
| Step | Action |
| 1 | At the project site, set up the Pave-IR system and verify system operation according to the unit instructions. Set the outer infrared sensors no closer than 1 ft and no further than 2 ft from the outer HMA edge. |
| 2 | Document the mix type, contractor, haul distance, target placement temperature, and brief description of placement operation. |
| 3 | Collect a thermal survey over a distance of 150 ft, or the distance of two truckloads, whichever is greater. Record the limits of the survey by stationing and/or GPS. Observe the following guidelines for collecting data: <ul style="list-style-type: none"> • Set Pave-IR to collect a transverse scan every 2 inches. • The infrared temperature bar should be no more than 8 ft behind the screed. • Document the location of any paver stops for reference. |
| 4 | View the collected thermal profile with the Pave-IR software. Display the analysis bar along with the thermal profile according to the following guidelines: <ul style="list-style-type: none"> • Set the target mat placement temperature as the target temperature in Pave-IR. |

| | |
|----|--|
| | <ul style="list-style-type: none"> Set the target range in Pave-IR at ± 25 °F from the target temperature. |
| 5 | Locate and annotate the areas of hottest temperatures on the thermal profile by pressing <CTRL> concurrently with the left mouse button. |
| 6 | Locate and annotate the areas of the coldest temperatures on the thermal profile. Specifically, locate and annotate areas that are 25 °F or more cooler than the hottest measured temperature. |
| 7 | Annotate the location of any paver stops on the thermal profile. |
| 8 | Create the histogram of temperature distributions within the survey limits using the Pave-IR bar chart function. |
| 9 | For the section under test (minimum length 1000 ft) locate 4 “cold spots” where the spot temperature is more than 25 °F below the target temperature. Mark these spots with paint spots. |
| 10 | Complete rolling of the test strip. |
| 11 | Remove two cores from each of the cold spots, and return them to the laboratory for density testing. |

Section 5. Reporting

Report the following information from the thermal imaging survey:

- Project description, including mix type, contractor, haul distance, target placement temperature, and brief description of placement operation.
- Station or GPS limits of the survey.
- Thermal plot produced by the survey, including Analysis Bar, annotated locations of the hottest and coldest locations, and annotated locations of any paver stops.
- Histogram of temperatures from the survey.
- Density of cores taken from “cold spots.”

-

